









# NAVAL POSTGRADUATE SCHOOL

## Monterey, California



# THESIS

C24435

Surface Circulation Associated with the Mindanao  
and Halmahera Eddies

by

Glen H. Carpenter

June 1989

Thesis Advisor:

Curtis Collins

Approved for public release; distribution is unlimited

Prepared for:  
Chief of Office of Naval Research  
800 North Quincy  
Arlington, VA 22217-5000

T244047

NAVAL POSTGRADUATE SCHOOL  
Monterey, California

Rear Admiral R.C. Austin  
Superintendent

Harrison Shull  
Provost

This report was prepared in conjunction with Chief Office of Naval Research, Arlington, VA and funded by the Naval Postgraduate School.

## REPORT DOCUMENTATION PAGE

1a Report Security Classification, Unclassified		1b Restrictive Markings	
2a Security Classification Authority		3 Distribution Availability of Report Approved for public release; distribution is unlimited.	
2b Declassification Downgrading Schedule		5 Monitoring Organization Report Number(s)	
4 Performing Organization Report Number(s) NPS-68-89-005		7a Name of Monitoring Organization Office of Naval Research	
6a Name of Performing Organization Naval Postgraduate School	6b Office Symbol (if applicable) 52	7b Address (city, state, and ZIP code) 800 Quency, Arlington, VA 22217-5000	
6c Address (city, state, and ZIP code) Monterey, CA 93943-5000		9 Procurement Instrument Identification Number ONN, Direct Funding	
8a Name of Funding Sponsoring Organization Naval Postgraduate School	8b Office Symbol (if applicable)	10 Source of Funding Numbers	
8c Address (city, state, and ZIP code) Monterey, CA 93943-5000		Program Element No	Project No
		Task No	Work Unit Accession No
11 Title (include security classification) SURFACE CIRCULATION ASSOCIATED WITH THE MINDANAO AND HALMAHERA EDDIES			
12 Personal Author(s) Glen H. Carpenter			
13a Type of Report Master's Thesis		13b Time Covered From To	14 Date of Report (year, month, day) June 1989
			15 Page Count 121
16 Supplementary Notation The views expressed in this thesis are those of the author and do not reflect the official policy or position of the Department of Defense or the U.S. Government.			
17 Cosati Codes		18 Subject Terms (continue on reverse if necessary and identify by block number)	
Field	Group	word processing, Script, GML, text processing.	
	Subgroup		
19 Abstract (continue on reverse if necessary and identify by block number) During June and July, 1988, an AXBT survey was conducted southeast of Mindanao, Philippines in conjunction with CTD sections completed along the coast of Mindanao. Simultaneously, six Lagrangian drifters are launched in the Mindanao Current. Analysis of the data indicate a highly dynamic and complicated circulation which forms the origin of the North Equatorial Countercurrent. Strong shears are observed across the Mindanao current and across a current located on the northeast coast of Borneo, and based on water mass characteristics and Lagrangian data, the general positions and strengths of the Mindanao and Halmahera Eddies.			
20 Distribution Availability of Abstract <input checked="" type="checkbox"/> unclassified unlimited <input type="checkbox"/> same as report <input type="checkbox"/> DTIC users		21 Abstract Security Classification Unclassified	
22a Name of Responsible Individual Curtis A. Collins		22b Telephone (include Area code) (408) 646-2768	22c Office Symbol 54Ss

Approved for public release; distribution is unlimited.

Surface Circulation Associated with the Mindanao  
and Halmahera Eddies

by

Glen H. Carpenter  
Lieutenant Commander, United States Navy  
B.S., University of Washington, 1977

Submitted in partial fulfillment of the  
requirements for the degree of

MASTER OF SCIENCE IN OCEANOGRAPHY AND METEOROLOGY

from the

NAVAL POSTGRADUATE SCHOOL  
June 1989

## ABSTRACT

During June and July, 1988, an AXBT survey was conducted southeast of Mindanao, Philippines in conjunction with CTD sections completed along the coast of Mindanao. Simultaneously, six Lagrangian drifters are launched in the Mindanao Current. Analysis of the data indicate a highly dynamic and complicated circulation which forms the origin of the North Equatorial Countercurrent. Strong shears are observed across the Mindanao current and across a current located on the northeast coast of Borneo, and based on water mass characteristics and Lagrangian data, the general positions and strengths of the Mindanao and Halmahera Eddies.

170015  
2635  
C.1

## TABLE OF CONTENTS

I. INTRODUCTION .....	1
II. BATHYMETRY .....	5
III. LAGRANGIAN DRIFTER MEASUREMENTS .....	8
A. MINI-TRISTAR DRIFTER .....	8
B. DRIFTER MEASUREMENTS .....	8
C. LAGRANGIAN TRAJECTORIES .....	9
1. Buoys launched along 7°N .....	11
a. Buoy 52 .....	11
b. Buoy 51 .....	13
c. Buoy 55 .....	13
2. Buoys launched along 8°N .....	18
a. Buoy 50 .....	18
b. Buoy 54 .....	20
c. Buoy 53 .....	20
D. LAGRANGIAN VELOCITY CORRELATIONS .....	21
1. Philippine Sea .....	23
2. Celebes Sea .....	25
E. LAGRANGIAN TEMPERATURES .....	26
F. SUMMARY .....	30
IV. AXBT AND CTD MEASUREMENTS .....	38
A. VERTICAL PROFILES .....	38
B. VERTICAL SECTIONS .....	39
C. HORIZONTAL TEMPERATURE STRUCTURE .....	42
D. DYNAMIC STRUCTURE .....	43
V. SUMMARY AND RECOMMENDATIONS .....	50
A. SUMMARY .....	50
B. RECOMMENDATIONS .....	51



## LIST OF TABLES

Table 1.	DRIFTER NECROLOGY .....	13
Table 2.	TIME AVERAGED LAGRANGIAN MEAN VELOCITIES .....	37
Table 3.	LAGRANGIAN VARIANCES AND EDDY KINETIC ENERGY ...	37
Table 4.	DYNAMIC HEIGHT COMPARISONS .....	43

## LIST OF FIGURES

Figure 1. Bathymetric Chart of the Survey Region .....	7
Figure 2. MINI-TRISTAR Drogue and Surface Float Configuration .....	10
Figure 3. Schematic of the Observed Motion of TRISTAR in Surface Waves ...	11
Figure 4. Geometry of Location Calculations .....	12
Figure 5. Lagrangian Trajectory of Buoy 52 .....	14
Figure 6. Buoy 52 Velocity Time Series .....	15
Figure 7. Lagrangian Trajectory of Buoy 51 .....	16
Figure 8. Buoy 51 Velocity Time Series .....	17
Figure 9. Lagrangian Trajectory of Buoy 55 .....	18
Figure 10. Buoy 55 Velocity Time Series .....	19
Figure 11. Lagrangian Trajectory of Buoy 50 .....	21
Figure 12. Buoy 50 Velocity Time Series .....	22
Figure 13. Lagrangian Trajectory of Buoy 54 .....	23
Figure 14. Buoy 54 Velocity Time Series .....	24
Figure 15. Lagrangian Trajectory of Buoy 53 .....	25
Figure 16. Buoy 53 Velocity Time Series Day 206-270 .....	26
Figure 17. Lagrangian Trajectory of Buoy 53 .....	27
Figure 18. Buoy 53 Velocity Time Series Day 270-350 .....	28
Figure 19. Buoy 53 Velocity Time Series Day 340-430 .....	29
Figure 20. Buoy 51 Lagrangian Velocity Correlations .....	30
Figure 21. Buoy 52 Lagrangian Velocity Correlations .....	31
Figure 22. Buoy 52 Lagrangian Velocity Correlations .....	32
Figure 23. Buoy 53 Lagrangian Velocity Correlations .....	33
Figure 24. Buoy 53 Lagrangian Velocity Correlations .....	33
Figure 25. Buoy 50 Lagrangian Velocity Correlations .....	34
Figure 26. Buoy 54 Lagrangian Velocity Correlations .....	34
Figure 27. Buoy 55 Lagrangian Velocity Correlations .....	35
Figure 28. Lagrangian Daily Minimum Sea Surface Temperature .....	36
Figure 29. AXBT and CTD Station Locations .....	39
Figure 30. Vertical Profiles of Temperature, Salinity, and Density Anomaly .....	40
Figure 31. Vertical Profile of Temperature, Salinity, and Density Anomaly .....	41

Figure 32. Vertical Temperature Cross-section A .....	44
Figure 33. Vertical Temperature Cross-section B .....	45
Figure 34. Vertical Temperature Cross-section C .....	46
Figure 35. 23° Isotherm .....	47
Figure 36. 14° Isotherm .....	47
Figure 37. 14°-23° Thickness .....	48
Figure 38. Buoy Trajectory composite .....	48
Figure 39. Dynamic Heights 0, 300 m .....	49

## I. INTRODUCTION

On January 1, 1985, the international TOGA (Tropical Ocean Global Atmosphere) program commenced. Planning for this program had been on going since 1981 with its central focus being air-sea interaction and its effect on the global climate. In 1982-1983, a strong El Nino event stimulated higher levels of interest in this research. TOGA is envisioned to be a 10-year program with its efforts centered around four major program elements. The first of these elements is modeling with an aim at fixing the predictability of the atmosphere through coupled air-ocean models. Second, empirical studies, based on historical data sets, will continue to contribute to the understanding of the processes that control the predictability of the environment. Third, process studies will be focused on those physical mechanism which are identified to be of critical importance to the understanding of large scale atmospheric - oceanographic variability. Finally, long term observations are necessary to determine the time-dependent structure of the tropical oceans and the global atmosphere.

Although, global effects of tropical air-sea interactions is central to the understanding of the circulation of the oceans at low latitudes along the western boundaries, yet until recently there had been few modern oceanographic observations in the western equatorial Pacific. Then, between 1985 and 1988, under the umbrella of the process studies element of TOGA, several expeditions were carried out as part of a Western Equatorial Pacific Ocean Circulation Study (WEPOCS). The third of these expeditions was a survey conducted by the *R/V Moana Wave* called WEPOCS III. The purpose of this cruise was [Lukas, et al, 1987]:

1. defining the circulation of the low-latitude western boundary currents of the western Pacific, including the possible cross-equatorial transports,
2. determining the convergence of waters of northern and southern hemisphere origin in the far western equatorial Pacific,
3. determining the source water mass characteristics for the Pacific to Indian Ocean Indonesian throughflow,
4. defining the Origin of the Equatorial Undercurrent, and
5. determining the circulation patterns which supply the North Equatorial Counter-current near its origin.

In order to learn more about the mesoscale structure in the region, the Naval Postgraduate School (NPS) supplemented the WEPOCS III program by providing ad-

ditional drifting buoys and an aircraft survey. Mini-TRISTAR drifting buoys were deployed to bracket the Mindanao Current. During three days in July, 1988, an Airborne Expendable Bathythermograph (AXBT) survey was conducted by NPS southeast of Mindanao, in which 84 temperature profiles were obtained. The data from these surveys are used in this study.

Prior to TOGA and WEPOCS, our understanding of the circulation of the region had been based on ship drift reports and inferences based on water mass properties [Wyrski, 1961 and Wyrski et al., 1976]. The precision and accuracy of ship drift estimates is well known to be limited. Errors in ship positioning also limit the accuracy of these estimates. Wyrski notes (1961) "The individual observation is an average over a period of 1 day and over a distance of about 400 km, somewhat larger than the typical midocean eddy, or the typical width of strong currents. The current speeds reported are consequently biased toward lower values. Included in the observed drift is also an undetermined effect of wind on the ship, which largely depends on the loading characteristics of the particular ship,"

There have been several research cruises to the region. The sections made by the *Kagoshi-maru* (1952) and the *Keiten-maru* (1954-1956) were very effective at resolving a cyclonic vortex east of Mindanao, called the Mindanao Eddy [Takahashi, 1959]. Sections made by the *Atlantis II*, at approximately 7°N and 8°N, and the survey conducted by the *Takuyo* (1965-1966) were effective in resolving the structure of the Mindanao Current. From an analysis of this data, Cannon [Cannon, G. A., 1965] concludes "The offshore limit of continuous strong currents is 70-80 km. Geostrophic surface currents and the ships set are consistent near Mindanao. The transport and the depth of the currents are different on the two sections, which were only about 100 km apart." Since these expeditions took place before mesoscale eddies had been "discovered", they were not designed to adequately resolve eddies. These earlier investigations did not make direct measurements of ocean currents.

The general circulation of the region has been described by Wyrski [Wyrski, 1961]. The description that follows is for Juno and is based on his monograph. The North Equatorial Current (NEC) approaches the northeast coast of Mindanao from the east and bifurcates into a northern flowing branch and a southern flowing branch. The southern branch, running from approximately 10°N to 3°N, is the Mindanao Current. The Mindanao Current flows along the coast of Mindanao, and at its southern tip, also splits into two branches. One branch flows southwestward over the ridge connecting Celebes and Mindanao (Celebes-Mindanao Ridge) while the second branch continues

southward along the ridge. The South Equatorial Current (SEC) also approaches from the east along the northern New Guinea coast and at the northwest tip of New Guinea separates into two branches. The northern branch then retroflects into the North Equatorial Countercurrent (NECC). The second branch continues on between New Guinea and Halmahera until it reaches the Island of Ceram where a second bifurcation takes place, with one branch entering the Banda Sea and the other flowing northward into the Molucca Sea. This latter branch eventually enters the Pacific Ocean through the Molucca Passage, converges with the southward flowing Mindanao Current, and retroflects into the NECC.

The southwest flowing extension of the Mindanao current which enters the Celebes Sea diverges into three separate extensions. The northern extension is very broad and passes through the Sulu Archipelago and into the Sulu Sea. The main extension passes through the central Celebes Basin and into the Java Sea via the Macassar Strait. The third extension is a retroflection of the current along the Celebes Peninsula which passes back over the ridge connecting Celebes and Mindanao between Celebes and the Island of Sangihe. This extension flows into the convergence zone of the Mindanao Current and the SEC.

Using water mass characteristics, and circulation patterns, Wyrski [Wyrski, 1961] suggested the presence of semi-permanent eddy features east of Mindanao (Mindanao eddy) and south of Mindanao (Halmahera Eddy). The exact size of these features is not well resolved although the radius is expected to be consistent with the Rossby radius measured in the region of 400 km [Emery, et al., 1984]. The Mindanao eddy is located east of Mindanao at approximately 7°N, 130°E and is associated with the reversal of flow of the North Equatorial Current (NEC), the Mindanao Current and the NECC. The Halmahera Eddy is located at 3°N, 133°E and is associated with the convergence of the SEC and the NECC.

This is a study of the physical oceanography of the region southeast of Mindanao and the flow of the Mindanao current into the Celebes Sea. The strategic importance of this region has been well documented and the effects of mesoscale eddies on anti-submarine warfare cannot be overstated. For these reasons the circulation characteristics described in this study will be important to naval operations. The basis for this study will be the six TRISTAR Lagrangian buoys launched in the vicinity of the Mindanao Current, and the AXBT and CTD data collected in the region by the R/V *Moana Wave*. This study will be primarily descriptive in nature and limited to the summer regime, as revealed by these data. Horizontal and vertical temperature character-

istics for the June-July (southwest monsoon) time frame for the region southeast of Mindanao will be discussed. Also included will be circulation patterns as determined by drifting buoys for the entire region from east of Mindanao to the Macassar Strait.

## II. BATHYMETRY

This study involves the throughflow of water between basins and would not be complete without a review of the bathymetry that helps to govern the flow. Although Wyrcki [Wyrcki, 1961] provides a very thorough discussion on the bathymetry of the region of this study, his discussion includes all southeast Asian waters. Since bathymetry, topography play such an important role in the magnitude and direction of ocean currents and eddies, a more detailed discussion is provided here. To avoid numerous references to Wyrcki, quotations will be used. Fig. 1, adapted from Wyrcki (1961) is a depiction of the bathymetry of the region.

South of Mindanao is the Molucca Basin. Its boundaries are defined by a series of ridges running between Mindanao, Halmahera, New Guinea, and Celebes. "The bottom of the basin is divided into five smaller basins which have depths between 3400 m and 4800 m." The Molucca Basin is closed on the east by a ridge running between Halmahera and Mindanao with a sill depth of 2340 m. To the south, the boundary of the basin is defined by a ridge running between Celebes and New Guinea containing the islands of Taliabu, Mangole and Obi. "The deepest threshold through this ridge is the Lifamatola Strait (located between Mangole and Obi) with a sill depth of 1800 m, which governs the replacement of the bottom water of all basins south of it." Completing the closure of the Molucca Basin is a ridge connecting the Celebes Peninsula with the southern tip of Mindanao. This ridge includes the islands of Siau and Sangihe and has a controlling sill depth of around 1400 m.

Further to the west of the Molucca Basin is the Celebes Basin which has as its eastern boundary the ridge connecting Mindanao and Celebes. This basin is relatively flat and has a maximum depth of 6220 m. The northern boundary of the Celebes basin is the Sulu Archipelago; "this is very shallow in large areas and consists of numerous coral banks." "Two channels, one east of Jolo with a sill of about 200 m depth, and another east of Sibutu, with a sill of about 270 m depth, form slightly deeper but very narrow thresholds." The western boundary of the Celebes Basin is the east coast of Borneo and the closure is completed in the south by the Celebes Peninsula.

Providing for the passage of water out of the Celebes Sea, to the south, is the Macassar Strait. Located between Borneo and Celebes, the central trench through this passage is around 2300 m in depth.

The Philippine Basin, located to the east of Mindanao and to the north of New Guinea, is the region of the Mindanao eddy. Separated from the New Caroline Basin to the south by a ridge running from Halmahera through the Palau Islands to Yap, its deepest depths of 10,000 m are found in the Philippine trench. Located at approximately 8.5°N, 131°E is a seamount which shoals to a depth of 3000 m.

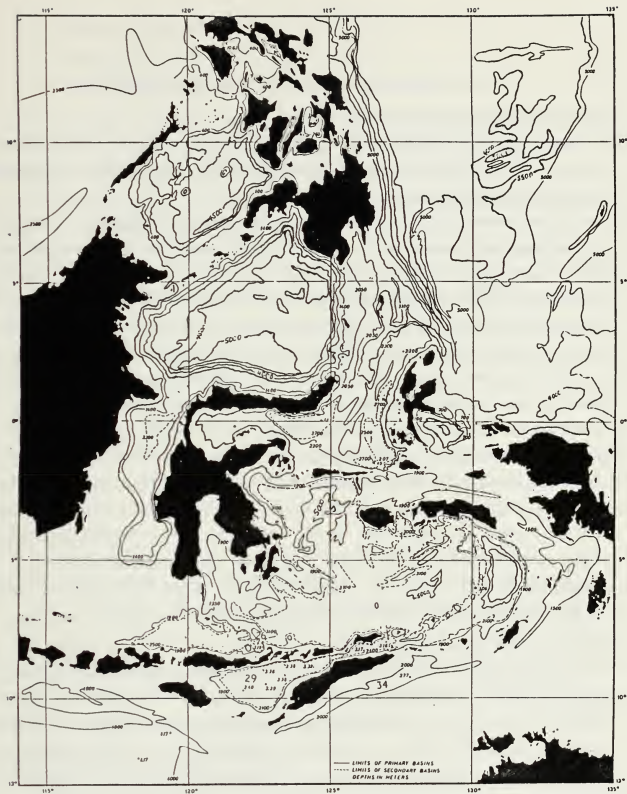


Figure 1. Bathymetric Chart of the Survey Region: (adapted from Wyrski, 1961)

### III. LAGRANGIAN DRIFTER MEASUREMENTS

#### A. MINI-TRISTAR DRIFTER

The data used in this study is a combination of temporal and spatial data and, as mentioned earlier, consists of drifters, AXBTs and CTDs. Here we discuss the measurements made by the surface drifting buoys.

Since a measurement of surface currents was desired, it was important to use a surface drifting buoy (subsequently called a "drifter") which would closely couple to the surface waters and minimize the effects of wind and waves. The buoy chosen is called a Mini-Tristar (Fig. 2) and was manufactured by Techocean Associates. The drifters feature small spherical surface and subsurface floats and a large symmetrical drogue in the shape of a corner-radar reflector [Poulain et al., 1987]. The surface float was designed to remain on the surface at least 80% of the time, while the subsurface float was designed with only weak negative buoyancy. This combination allowed slack to develop in the cable which connected these two floats. This would allow the drogue to move horizontally through the water with the vertical motion of the surface float decoupled from the horizontal subsurface motion. However, under strong wave forcing the surface float was observed to submerge (both in field tests and in a laboratory wave tank). The resulting buoyant force of the surface float would "take up" the slack in the line causing a dramatic vertical oscillation of the drogue (Fig. 3), as the floats become coupled. Fortunately, the slippage is minimal. A detailed discussion of the characteristics and design of the TRISTAR drifters is given by Niiler (1987) [Niiler, et al., 1987].

#### B. DRIFTER MEASUREMENTS

The buoys were tracked from two polar-orbiting NOAA satellites, using a system called ARGOS. The ARGOS system has been described by Poulain. [Poulain et al., 1987, p. 3]. "Positions were determined from Doppler-shifted radio signals. The field of possible positions for a buoy is in the form of a half-cone (Fig.4) with the satellite at its apex, the satellite velocity vector as axis of symmetry, and the apex half-angle ( $A$ ) such that:

$$\cos(A) = [(f_r - f_e) \cdot f_e] \times c / V$$

where:

$$c = \text{speed of light}$$

$V$  = satellite speed relative to buoy

$f_e$  = transmission frequency, and

$f_r$  = receive frequency.

The intersections of the various location cones with the ocean surface gives two possible positions of the buoy. Additional information - previous locations, range of possible speeds - is required to find which of the two positions is correct."

The location quality of the fixes received from service ARGOS was based on the length of the satellite pass, the control over oscillator stability, geometric conditions, and how rapid the convergence of the fix was in the least-squares computation. The conditions encountered during this study provided, in most cases, a 68% confidence interval that the fix was accurate to within 350 m. In many instances the fixes were accurate to within 150 m. Accordingly, the position data required only manual smoothing by removing obviously bad fixes. This was done by plotting the trajectories using the raw data and then eliminating those fixes which were clearly in error. In one instance, Buoy 53, a simple 5 point triangular filter was used to adequately resolve the initial recirculation it underwent in the Mindanao Eddy during the first month of the record. Additionally, due to problems with the buoy transmit terminal oscillator, approximately eight days of record were lost in the early part of Buoy 51's record. The temperature and submergence time of the buoys was also collected and were filtered using a cosine running mean filter.

Initial processing of drifter data was done by service ARGOS. They provided monthly data tapes which contained location data as well as temperature and submergence records. The buoys in the study averaged 5.1 fixes per day. For each of the location fixes the quality was determined by service ARGOS. To obtain positions at standard times a linear interpolation was used on the position data to obtain positions every twelve hours. Velocity time series were obtained from these interpolated positions and then smoothed using a 2.5 day running mean filter.

### C. LAGRANGIAN TRAJECTORIES

The buoys were launched on 16 July and between 22 and 23 July, 1988. The longest and shortest records were 209 and 17 days, respectively, with an average record length of 70 days. In order to obtain measurements of the shear across the Mindanao Current, buoys were launched along lines perpendicular to the current at 8°N and 7°N, with the position of the current determined by shipboard measurements. Table 1 lists the exact

## Ministar Lagrangian Drifter

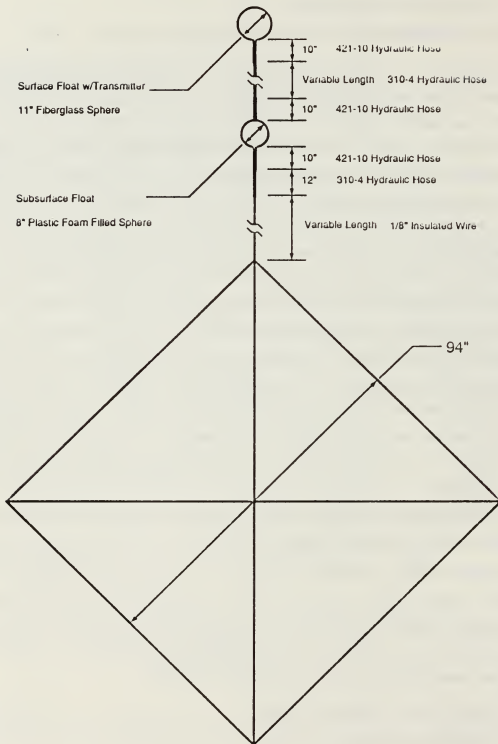


Figure 2. MINI-TRISTAR Drogue and Surface Float Configuration

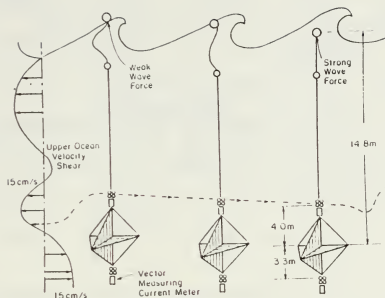


Figure 3. Schematic of the Observed Motion of TRISTAR in Surface Waves: (from Niiler, et al., 1987)

dates and locations of launch in addition to the record length of each buoy and their failure mode.

# 1. Buoys launched along 7°N

## a. Buoy 52

Buoy 52 was launched on 16 July about 17 km east of Tugubun Pt. on the south east corner of Mindanao in approximately 4500 m of water (Figs. 5 and 6). Its initial trajectory was to the southwest at a speed of 100 cm/s. By 19 July (Julian 200) it had slowed to 40 cm/s as it began to pass over the Celebes-Mindanao Ridge. In moving over the ridge, the water depth shallows to a minimum of 180 m. Then, on 20 July, it backs to the southeast, nearly running aground on the small island of P Kawalusu located at 4.3°N, 125.4°E. On 22 July the buoy was established in a recirculation pattern

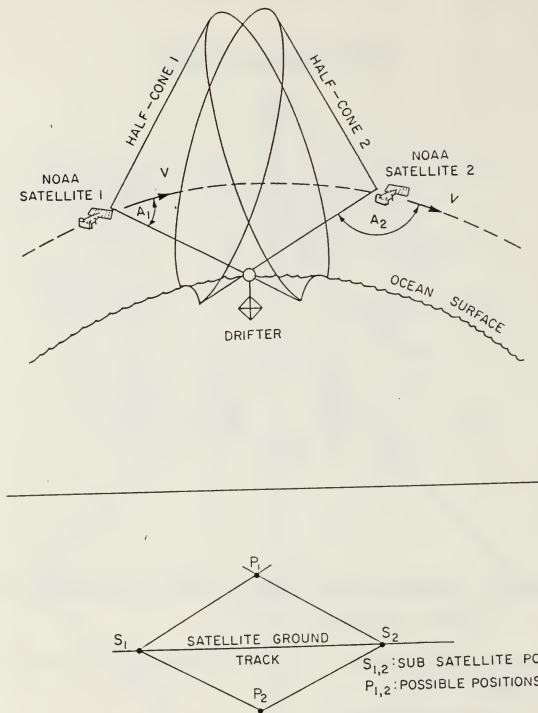


Figure 4. Geometry of Location Calculations: (from Poulain et al., 1987)

to the northeast and passed 22 km northeast of Sangihe through 150 m of water. The buoy then continued toward the island of P Karakelong, then rapidly backed further to the north until it cleared the island on 28 July (Julian 209). Upon island passage, the buoy veered eastward and continued its drift into the NECC, and then accelerated to 120 cm/s, the largest speeds observed by this which were the largest speeds observed by this buoy. It then recurred to the southeast, slowing to 115 cm s. On 1 August (Julian 213)

Table 1. DRIFTER NECROLOGY

BUOY	Date of launch	Location of launch	Record length	Failure mode
Buoy 50	23 July 88	7.958°N 126.556°E	48 days	Lost Drogue
Buoy 51	16 July 88	6.983°N 127.304°E	33 days	Lost Drogue
Buoy 52	16 July 88	6.944°N 126.619°E	53 days	Lost Drogue
Buoy 53	22 July 88	7.983°N 127.958°E	220 days	Grounded
Buoy 54	22 July 88	7.990°N 126.975°E	17 days	Picked up at Sea
Buoy 55	16 July 88	6.861°N 126.861°E	63 days	Grounded

it entered an anticyclonic oscillation in the Philippine Sea. When the buoy reached 7°N, 134°E it slowed to 60 cm/s and began a cyclonic recirculation. It completed a 75 km radius gyre, maintaining 60 cm/s, by 23 August (Julian 235) and then began a second anticyclonic trajectory. A quarter of a period into this oscillation the buoy is lost on 17 September (Julian 260).

*b. Buoy 51*

Buoy 51 (Figs. 7 and 8) was launched on 16 July about 75 km east of Buoy 50. Its initial trajectory was to the south at 44 cm/s. On 18 July it began to slow to 20 cm/s. At this point, the buoy transmit terminal oscillator failed. The oscillator began functioning again on 28 July (Julian 209), and the buoy was located at 6.7°N, 129.4°E. The buoy began circulating to the south and east in a cyclonic pattern at 66 cm/s. It continued in this pattern until 19 August (Julian 231) when it slowed to 7 cm/s before sharply turning back to the west. The buoy was last tracked at 6.3°N, 133.6°E. It was lost on 20 August 88 (Julian date 232).

*c. Buoy 55*

Buoy 55 was launched on the axis of the Mindanao Current on 16 July and immediately began to drift to the southwest at a speed of 90 cm/s. Within 24 hrs it had passed within 5000 m of Cape Augustine and began to pass over the Celebes-Mindanao Ridge wherein it briefly maintained a speed of 80 cm/s (Figs. 9 and 10). By 22 July it

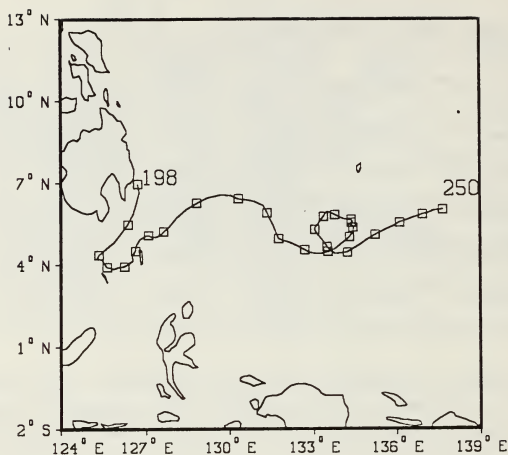


Figure 5. Lagrangian Trajectory of Buoy 52: Julian dates mark the beginning and end of each record and a square is placed as a marker for 12z every second day.

had cleared the ridge and began to slow. During one 24-hour period between 24 and 25 July, the speed dropped to as low as 2 cm/s. On 26 July the speed increased to 25 cm/s and the buoy began to drift back to the south, eventually completely retroflected back to the east and then drifted along the coast of the Celebes Peninsula, passing within 5000 m of landfall. It began to move back to the north on 15 August (Julian 227) and, after two days, along this track it turned sharply to the west. During this evolution, the buoy maintained a speed of 25-40 cm/s with the exception of a brief period on 17 August (Julian 229) when it slowed to 12 cm/s. By 19 August the buoy had completed an oscillation with a radius of 150 km, had accelerated to 80 cm/s and was moving toward the southwest extreme of the Sulu Archipelago. On 23 August (Julian 235) it passed within

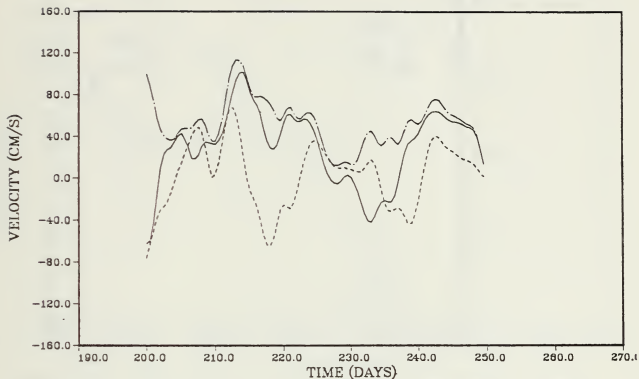


Figure 6. Buoy 52 Velocity Time Series: Velocities were calculated from interpolated trajectories and then filtered using a 2.5 day triangular running mean. The dashed line is the v component, the solid line is the u component and the chain-dot line is the modulus.

10 km of the Subutu Passage through the Archipelago but managed to maintain its trajectory around the Celebes basin. It eventually moved back to the south within 10 km of the coast of Borneo. On 31 August the buoy entered the Macassar Strait. On the day prior to entering the Strait, the buoy had reached its maximum sustained speed, 145 cm/s. Moving through the Macassar Strait, the buoy meandered along the 1400 m isobath with a wavelength of 500 km. During the last 5 days in which the buoy transited the Strait, it maintained a consistent 35 cm/s speed until it apparently lost its drogue,

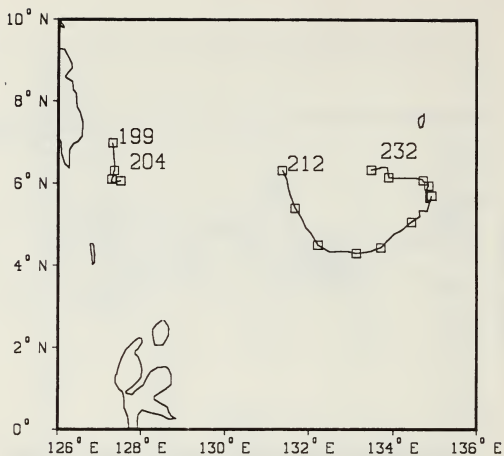


Figure 7. Lagrangian Trajectory of Buoy 51: Julian dates mark the beginning and end of each record and a square is placed as a marker for 12z every second day.

having either run aground or been trapped in fishing nets, on 18 September, as it was entering the Flores Sea.

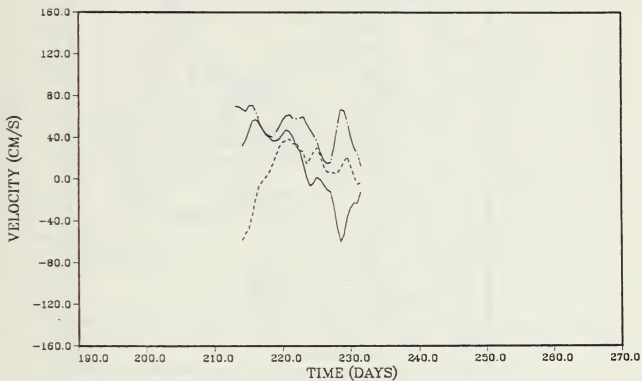


Figure 8. Buoy 51 Velocity Time Series: Velocities were calculated from interpolated trajectories and then filtered using a 2.5 day triangular running mean. The dashed line is the  $v$  component, the solid line is the  $u$  component and the chain-dot line is the modulus. Gap in record reflects failure of buoy transmit terminal oscillator.

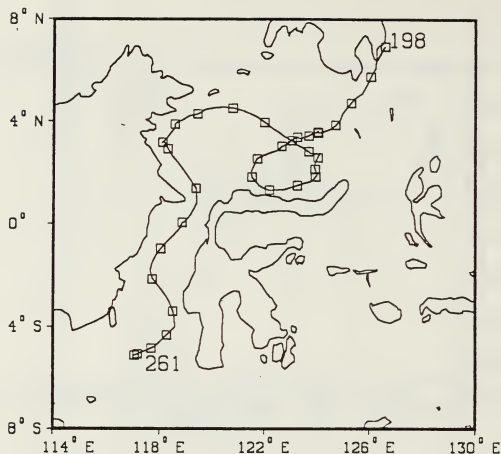


Figure 9. Lagrangian Trajectory of Buoy 55: Julian dates mark the beginning and end of each record and a square is placed as a marker for 12z every second day.

## 2. Buoys launched along 8°N

### a. Buoy 50

Buoy 50 was launched on 23 July, 14 km northeast of Bingai Pt. on Mindanao and moved to the south at 120 cm/s on the inshore side of the Mindanao Current. During its first day of drift, the buoy passed within 4000 m of Pusan Point and then continued to the south (Figs. 11 and 12). On 24 July, at approximately 6.9°N, 126.5°E, the buoy veered to the southeast and slowed slightly. On 25 July, the buoy began to drift farther to the southeast and passed Cape San Augustine 3500 m to the southwest. Continuing to the southwest, the speed varied from 40 to 50 cm/s as it passed over the Celebes-Mindanao Ridge at Sarangani Island in 180 m of water. For

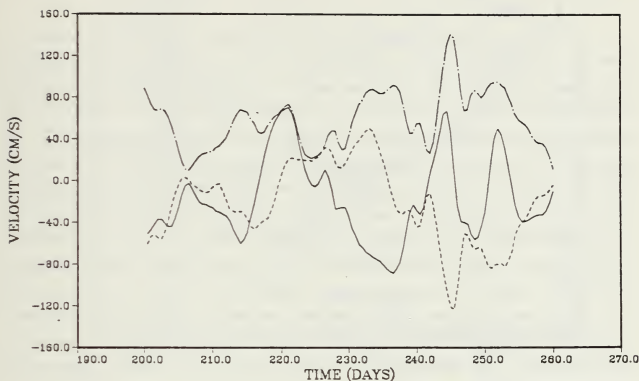


Figure 10. Buoy 55 Velocity Time Series: Velocities were calculated from interpolated trajectories and then filtered using a 2.5 day triangular running mean. The dashed line is the v component, the solid line is the u component and the chain-dot line is the modulus.

the next few days the buoy continued to move to the southwest with little variability in speed. Then on 3 August, the buoy slowed to 10 cm s as it entered a small cyclonic oscillation at 3°N, 122.5°E. Upon completing this rotation, the buoy moved to the northwest at 30 cm s on 8 August. The buoy approached within 100 miles of the Sulu Archipelago, and then turned to the southeast, following the 4000 m isobath.

As the buoy approached the entrance to the Macassar Strait, its velocity accelerated to 80 cm s. It passed the entrance on 30 August (Julian 242) and then passed

within 2000 m of the northern tip of Celebes wherein it turned northward into the Central Celebes Sea. Near 2°N, 121°E the buoy speed was 5 cm/s. The speed briefly increased to 16 cm/s two days prior to the buoy being lost on 11 September (Julian 254).

*b. Buoy 54*

Buoy 54 was launched on 22 July on the axis of the Mindanao Current, as determined by shipboard measurements (Figs. 13 and 14). It initially moved to the south with a speed of 80 cm/s. An interesting aspect of this buoy's trajectory can be made by comparing its movement with the movement of Buoy 52, which was launched 7 days earlier and to the southeast of Buoy 54's launch site. The relative positions of It was expected that, based on the relative positions of their two tracks, Buoy 54 to the north and west of Buoy 52, Buoy 54 would retroflect back to the northeast in a manner similar to Buoy 52. Contrarily, Buoy 54 continued over the Celebes-Mindanao Ridge at a speed between 50 and 70 cm/s. In the process of passing over the ridge, the water depth shoals to 150 m and the buoy passed within 1000 m of the small islands of P Kawio and P Kamboling, located 90 km north of Sangihe. By 25 July, the buoy accelerated to 100 cm/s and is continued along a path similar to the path of Buoy 50. When the buoy reached the central Celebes Sea, it had slowed to 50 cm/s, it was beginning to move to the south when it was picked up on 10 August (Julian 222) by a ship and taken to the southern coast of Mindanao.

*c. Buoy 53*

Buoy 53 was launched on 22 July, east of the Mindanao Current. This buoy has the longest record (220 days) and spent its entire time in the Philippine Sea (Figs. 15 through 19). Initially, it moved in a slow elliptical path, with the major and minor axis of this circulation 100 km and 50 km, respectively. It remained in this circulation for the first 42 days of its history moving at speeds between 10 and 40 cm/s with occasional accelerations to speeds as high as 70 cm/s. The center of this circulation was 7°N, 128.5°E and most likely captures the signature of the center of the Mindanao Eddy. On 2 September (Julian 245) the buoy began to move to the southeast and slowly accelerated to 80 cm/s. By 22 Sept, at which time it moved eastward in the NECC. With its speed as high as 50 cm/s to 100 cm/s, the buoy continued to the east reaching 141.7°E on 8 October. At this point it moved to the north, and then northwesterly. On 7 November (Julian 311) it had completed a retroflection to the west. It then traced out a 400 km wavelength oscillation to the north, with typical speeds of 25 to 30 cm/s, passing 200 km east of Palau, and entering the flow of the NEC. Once in the NEC it moved westerly, passing through a 650 km wavelength oscillation. Speeds in the NEC varied

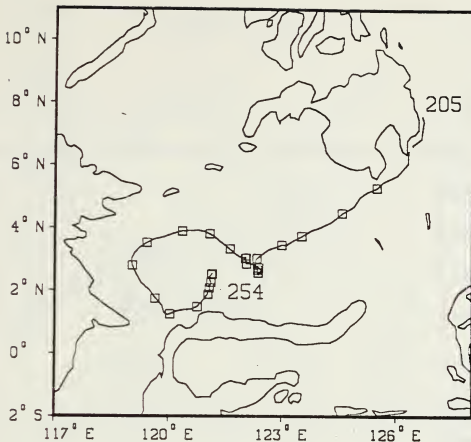


Figure 11. Lagrangian Trajectory of Buoy 50: Julian dates mark the beginning and end of each record and a square is placed as a marker for 12z every second day.

between 5 and 60 cm/s with the largest speeds at 11°N, 128°E. The buoy apparently drifted ashore or lost its drogue on the Island of Luzon on 26 February.

#### D. LAGRANGIAN VELOCITY CORRELATIONS

The velocity time series were linearly interpolated using a great circle solution. Similar to the method used by Poulain [Poulain, et al, 1987, pp. 4), the smooth (2.5-day running mean filter) velocity time series were used to calculate the mean velocities for each drifter. From the mean velocity, a residual velocity data set was computed and used to calculate the correlation functions. "Lagrangian time lagged velocity correlations were then computed by averaging time lagged velocity products from individual buoys." Using auto-correlation function and cross-correlation functions;

$$R(U)_{\tau} = E[U(t)U(t + \tau)]$$

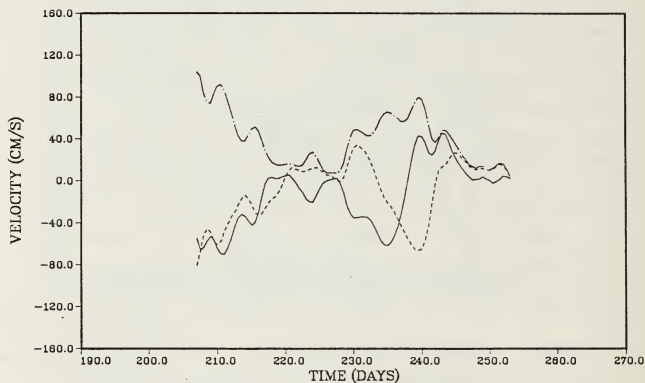


Figure 12. Buoy 50 Velocity Time Series: Velocities were calculated from interpolated trajectories and then filtered using a 2.5 day triangular running mean. The dashed line is the v component, the solid line is the u component and the chain-dot line is the modulus.

$$R(V)_\tau = E[V(t)V(t + \tau)]$$

$$R(UV)_\tau = E[U(t)V(t + \tau)]$$

$$R(VU)_{-\tau} = E[U(t)V(t - \tau)]$$

where  $\tau$  is the time lag. These functions are shown in Figs. 20 through 27 with redundant halves of the curves, due to symmetry, omitted. Using the velocity time series and

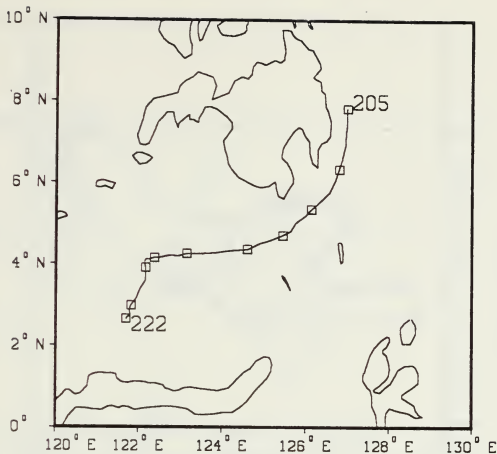


Figure 13. Lagrangian Trajectory of Buoy 54: Julian dates mark the beginning and end of each record and a square is placed as a marker for 12z every second day.

the correlation functions, Tables 2 and 3 were constructed to compare the mean velocities, variances and eddy kinetic energy (EKE) per unit mass of each buoy.

#### 1. Philippine Sea

Buoys 51, 52, and 53 remained in the Philippine Sea. Their Lagrangian velocity correlations (Figs. 20 thru 24) show that most of the differences discernible between these correlations are dependent upon their launch position and initial movement. Buoy 52 has the highest variance and energy associated with it, however; it was initially in the strong flow of the Mindanao Current. If the effects of the current are removed (Fig. 22), we see a correlation more closely resembling the other two buoys. (Figs. 20 and 21). This also leads to a velocity modulus of  $4.83 \text{ cm s}^{-1}$  which compare more closely to Buoys 51 and 53. For all buoys in the Philippine Sea, the energy is concentrated in the zonal

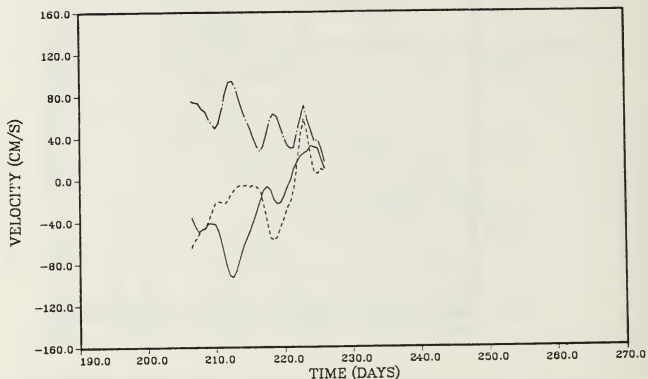
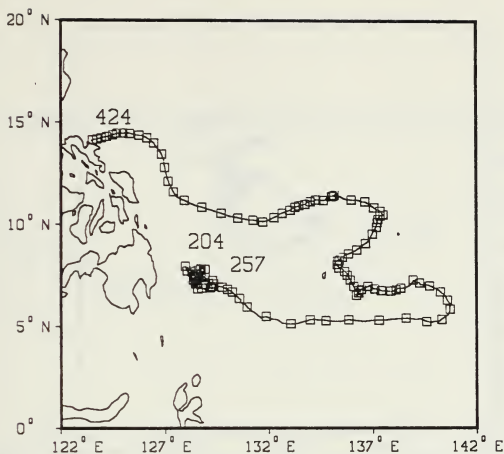


Figure 14. Buoy 54 Velocity Time Series: Velocities were calculated from interpolated trajectories and then filtered using a 2.5 day triangular running mean. The dashed line is the v component, the solid line is the u component and the chain-dot line is the modulus.

direction, even for Buoy 52 which was in the southwesterly flow of the Mindanao Current.

The most significant difference in time scales is that of Buoy 53, Fig. 23. The early part of this buoy's trajectory was trapped in a slow oscillation (probably the center of the Mindanao Eddy), with a time scale 30 days. However, if the early part of the record from this buoy's velocity time series is removed and the correlations (Fig. 24) re-



**Figure 15.** Lagrangian Trajectory of Buoy 53: Julian dates mark the beginning and end of each record and a square is placed as a marker for 12z every second day.

computed, the result is a time scale of the order of 10 days, which is exactly what was observed for Buoys 51 and 52.

## 2. Celebes Sea

Buoys 50, 54, and 55 all entered and remained in the Celebes Sea (Figs. 25 through 27). The slightly lower kinetic energy of Buoy 50 is associated with the small oscillation it undergoes between 3 August and 8 August. Regardless of this oscillation the total kinetic energy of the buoy is of the order of magnitude of Buoys 54 and 55. The energy of the buoys appears to be evenly distributed between the north-south and east-west planes with the exception of Buoy 54 which was picked up at sea just as it began a southward excursion. For all three cases in the Celebes Sea, the velocity time scales of ten days is the same as that found in the California Current system by Poulain (Poulain, et al., 1987).

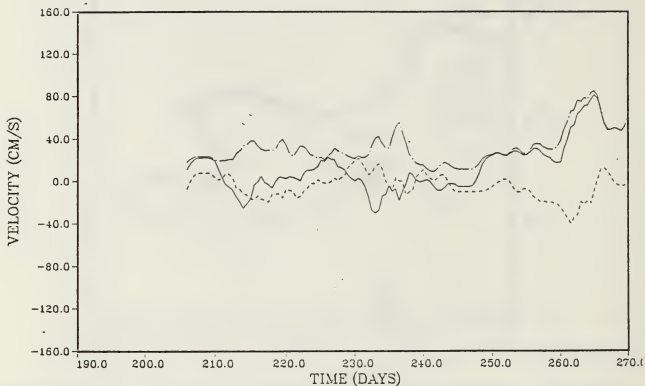


**Figure 16. Buoy 53 Velocity Time Series Day 206-270:** Velocities were calculated from interpolated trajectories and then filtered using a 2.5 day triangular running mean. The dashed line is the  $v$  component, the solid line is the  $u$  component and the chain-dot line is the modulus.

## E. LAGRANGIAN TEMPERATURES

Sea surface temperature was measured inside the surface float by a thermistor imbedded in a stainless steel bolt which passes through the shell of the float beneath the waterline. The measured temperature exhibited diurnal changes ranging from  $28^{\circ}\text{C}$  to  $33^{\circ}\text{C}$  (see Appendix B). It is not certain whether this diurnal variability is real or not. For example, on a calm day, the surface float might absorb more of the sun's radiation than the surrounding water. Since there was no way of compensating for differential

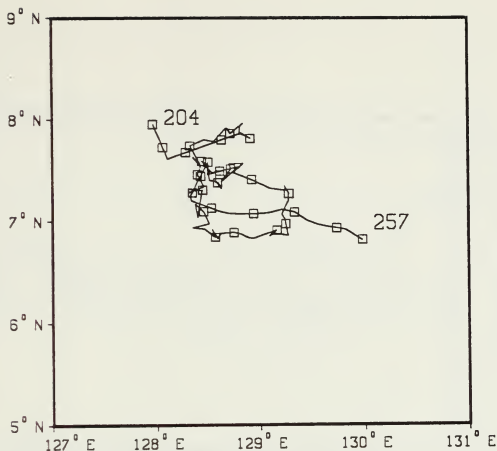


Figure 17. Lagrangian Trajectory of Buoy 53: First 53 days while in the Mindanao Eddy.

heating of the surface float and water, and my main interests were the larger scale, lower frequency patterns, an attempt to remove the diurnal variability was made. This was done by using only the mean minimum daily temperature for each buoy. On average this would be a record of the mean nighttime sea surface temperature and the diurnal effects would be filtered out. These temperature records as a time series are presented in Fig. 28. It should be kept in mind that the record is also a spatial series.

In general, the mean temperature variations between buoys is small. The temperature spread is usually between  $29^{\circ}\text{C}$  and  $29.5^{\circ}\text{C}$  especially between 7 August (Julian 219) and 29 August (Julian 241). However, most buoys experienced anomalous high and low temperatures. For example, Buoy 55 (launched on the inshore side of the Mindanao current) had an initial temperature of  $28.1^{\circ}\text{C}$ , considerably lower than the other buoys launched on the inshore side. This could be explained by deep water upwelling along the coast due to the prevailing southwest monsoon winds. The large drop in temperature of

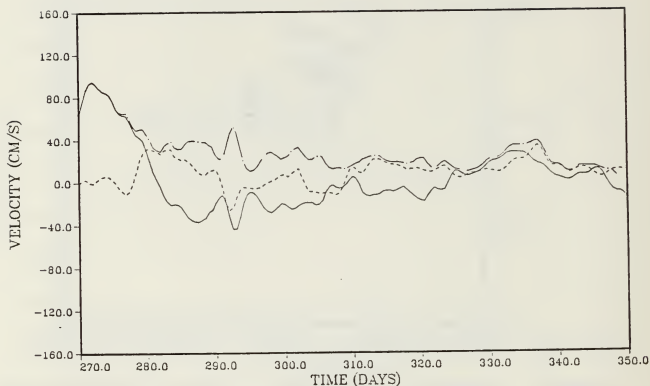


Figure 18. Buoy 53 Velocity Time Series Day 270-350: Velocities were calculated from interpolated trajectories and then filtered using a 2.5 day triangular running mean.

Buoy 52 (launched inshore and north of Buoy 55) as it drifted to the south, on 3 August, (Julian 215) also suggests the presence of colder water along the shore. Between August 16 (Julian 228) and August 28, Buoy 55 experienced unusually high temperatures of 29.5°C and 29.6°C. During these episodes, Buoy 55 also experienced brief but small accelerations in its speed. This suggests that the increased temperatures occur in conjunction with a strengthening of the temperature gradient in the Central Celebes Sea and along the coast of the Celebes Peninsula. On September 8 (Julian 251), as Buoy 55 is

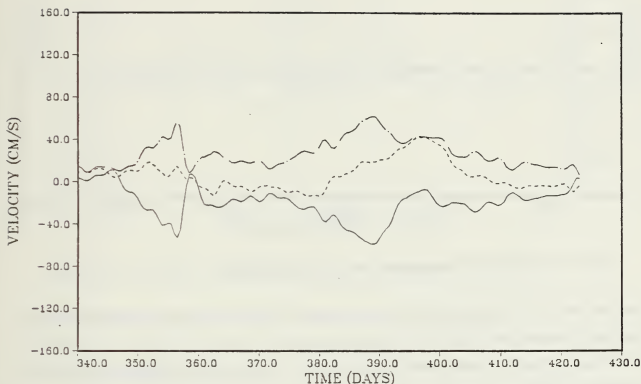


Figure 19. Buoy 53 Velocity Time Series Day 340-430: (Julian days greater than 366 are in reference to 1989). Velocities were calculated from interpolated trajectories and then filtered using a 2.5 day triangular running mean.

beginning to enter the Flores Sea, it experienced a rapid temperature decrease from  $29.4^{\circ}\text{C}$  to  $28.6^{\circ}\text{C}$ .

Between 27 July (Julian 208) and 1 August, Buoy 50 experienced a marked increase in temperature from  $29.5^{\circ}\text{C}$  to  $30.4^{\circ}\text{C}$ . At the same time, Buoy 50 accelerated from 30 cm/s to 50 cm/s and was located at  $4.2^{\circ}\text{N}$ ,  $124.5^{\circ}\text{E}$ . A speculative explanation for this marked increase in temperature and the concurrent acceleration could be that this lo-

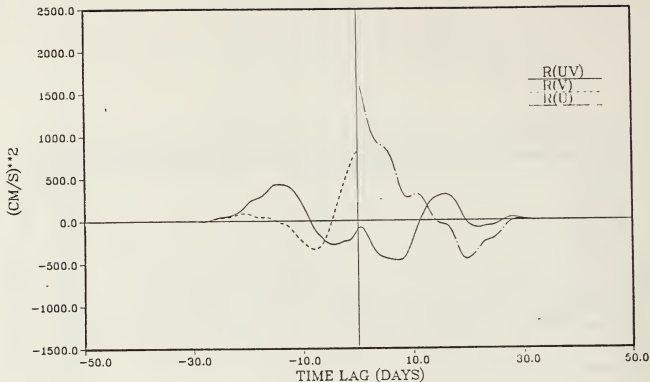


Figure 20. Buoy 51 Lagrangian Velocity Correlations

cation marks the boundary between the water mass of a south equatorial Pacific intrusion and the resident Celebes Sea water mass.

Buoys 52 and 53 both entered the NECC after separating from the influence of the Mindanao and Halmahera Eddies around 24 August (Julian 236) and immediately experienced a warming from 29.5°C to 30°C

showing that the core of the NECC is likely marked by a meridional temperature maximum. In both cases this warming is concurrent with accelerations in speed. In the case of Buoy 52, the speed increases from 30 cm/s to 80 cm/s by 29 August. Buoy 53 experienced minor warming episodes on 4, 12, and 17 September and in each case there was a concurrent acceleration between 5 and 10 cm/s.

## F. SUMMARY

It is difficult to generalize circulation patterns from only six drifters. Nevertheless, I will try to summarize these results. In relation to the Mindanao Current, three drifters were launched on the inshore side, two were launched on the seaward side, and one was launched on the axis. The buoys launched inshore or on the axis all moved initially towards the Celebes Sea at speeds in excess of 100 cm/s and with kinetic energy about 1000 (cm/s)<sup>2</sup>. While the buoys launched to the seaward side also had a high energy relative

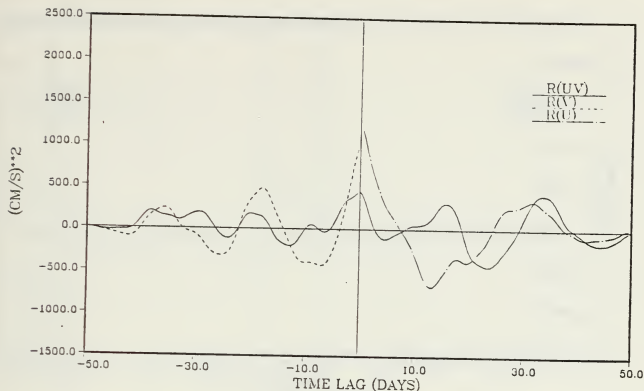


Figure 21. Buoy 52 Lagrangian Velocity Correlations: Days 198-248.

to midocean values, the energy was considerably less, ( $O(500)$ ), than the Mindanao Current. With the exceptions of Buoys 50 and 55, both launched inshore, the energy was predominately associated with the zonal flow. In the cases of Buoys 50 and 55, the energy was evenly distributed between zonal and meridional flow. The time-averaged mean velocities also reflect this distribution of energy. At the surface the Mindanao current was strong and narrow.

The trajectories of Buoys 50 and 55 suggest that the Celebes Sea was dominated by a large cyclonic gyre in the central basin and a strong southeasterly current along the coast of Borneo which bifurcates at the entrance to the Macassar Strait. Buoy 55 which reaches a maximum sustained speed of 145 cm s passed within 50 km of the coast of Borneo and then enters the Strait. Buoy 50 reached a maximum sustained speed of 80 cm s, approached the coast of Borneo 60 km further to the east, and then bypassed the entrance to the Strait and moved northward in the Celebes Sea. Surface flow into the Macassar Strait seemed to be restricted to waters close to shore and northwest of the Strait.

The trajectories east of Mindanao reveal three distinct circulations. The Mindanao eddy center was located at  $7^{\circ}\text{N}$ ,  $128.5^{\circ}\text{E}$ , as indicated by the initial trajectory of Buoy 53. Buoy 52 completes a anticyclonic oscillation "over the top" of the Halmahera Eddy

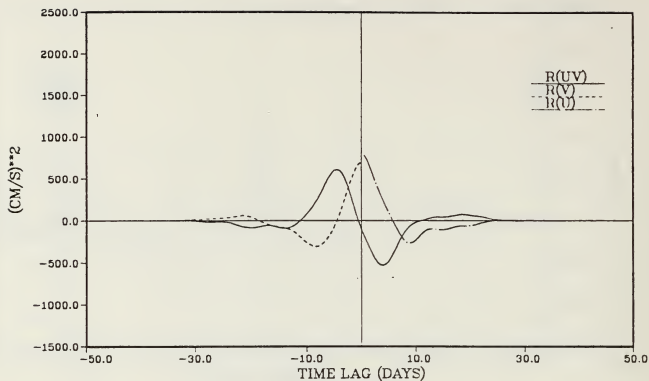


Figure 22. Buoy 52 Lagrangian Velocity Correlations: Days 220-250, computed after removing effects of the Mindanao Current

and then makes an additional cyclonic circulation further to the east revealing the complexity of the circulation associated with the origin of the NECC. The strongest flow was encountered at  $5^{\circ}\text{N}$ ,  $128^{\circ}\text{E}$ . This is a region of a front between SEC and NEC derived waters and will be discussed in the next section.

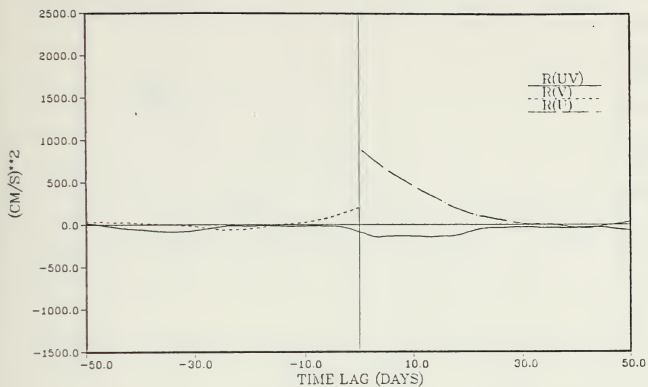


Figure 23. Buoy 53 Lagrangian Velocity Correlations: Days 204-424

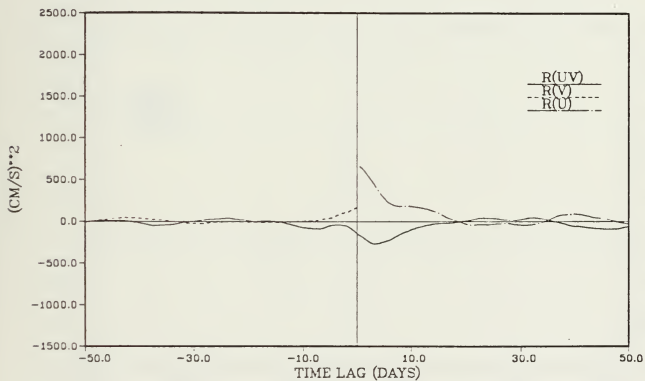


Figure 24. Buoy 53 Lagrangian Velocity Correlations: Computed after removing the effects of the Mindanao Eddy. Days 204-257.

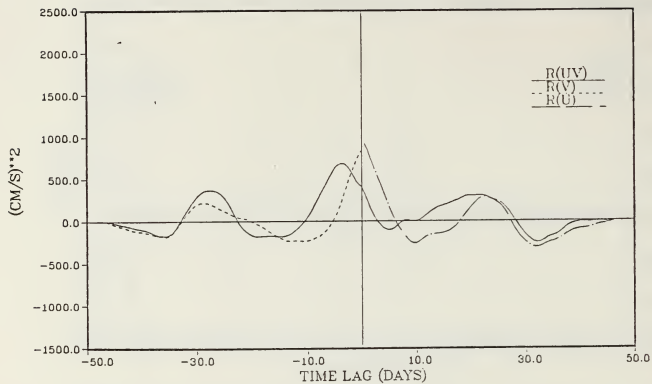


Figure 25. Buoy 50 Lagrangian Velocity Correlations

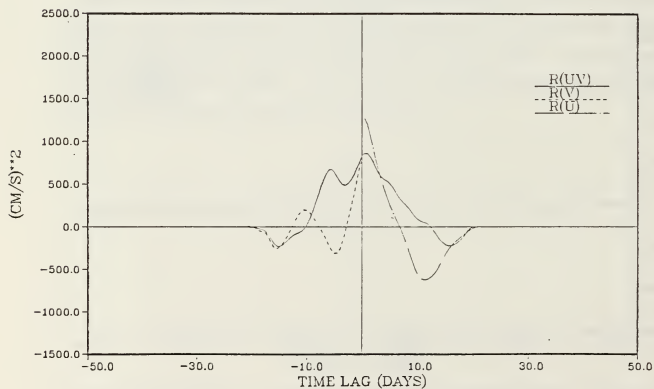


Figure 26. Buoy 54 Lagrangian Velocity Correlations

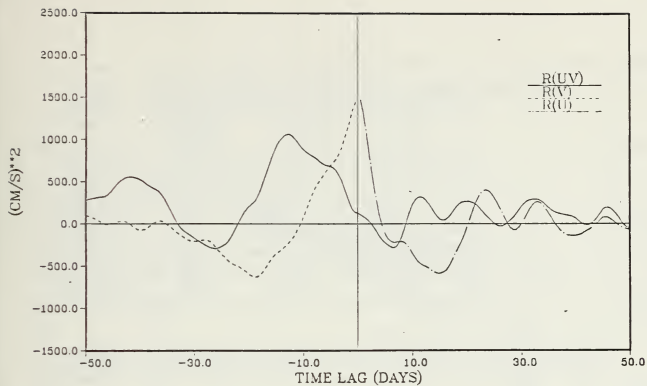


Figure 27. Buoy 55 Lagrangian Velocity Correlations

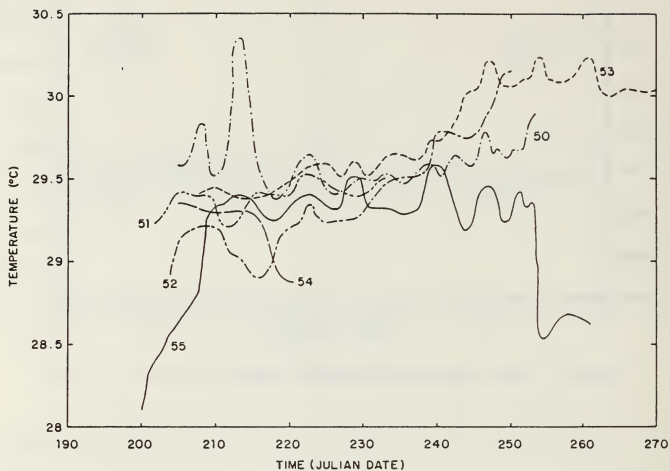


Figure 28. Lagrangian Daily Minimum Sea Surface Temperature

**Table 2. TIME AVERAGED LAGRANGIAN MEAN VELOCITIES**

BUOY	Mean U velocity (cm s)	Mean V Velocity (cm s)	Mean Speed (cm s)
Buoy 50	-13.9	-9.8	17.0
Buoy 51	5.4	-7.4	14.6
Buoy 52	29.4	2.2	29.5
Buoy 53	6.6	3.0	7.3
Buoy 54	-25.7	-16.4	30.5
Buoy 55	-18.6	-22.0	28.8

**Table 3. LAGRANGIAN VARIANCES AND EDDY KINETIC ENERGY**

Buoy	U Variance (cm/s) <sup>2</sup>	V variance (cm/s) <sup>2</sup>	U EKE (cm/s) <sup>2</sup>	V EKE (cm/s) <sup>2</sup>
Buoy 50	920	830	460	415
Buoy 51	1590	816	795	408
Buoy 52	1178	1002	589	501
Buoy 53	874	196	437	98
Buoy 54	1269	792	635	396
Buoy 55	1470	1476	735	738

#### IV. AXBT AND CTD MEASUREMENTS

The AXBT survey conducted by the Naval Postgraduate School in July, 1988 was confined to a region southeast of Mindanao. The zonal and meridional boundaries of the survey were  $1^{\circ}\text{N}$ - $7^{\circ}\text{N}$  and  $126^{\circ}\text{E}$ - $130^{\circ}\text{E}$ , respectively (Fig. 29). Areal coverage was limited by available flight time and equipment failure. The region was chosen to complement the ship survey and to further document the mesoscale variability. The processing of the 85 profiles used in this study was conducted at the Naval Postgraduate School. While 95% of the data could be adequately smoothed by linearly interpolating across bad data points, the remaining 5% required a cosine running mean filter for smoothing.

The CTD casts used in this study were collected during the second leg of the WEPOCS III cruise. Casts were made to the bottom or 4500 m depending on the local water depth. The first section occupied by the *R/V Moana Wave* was from  $7^{\circ}\text{N}$ ,  $134^{\circ}\text{E}$  to  $2.5^{\circ}\text{N}$ ,  $131.7^{\circ}\text{E}$ , with stations spaced half a degree of latitude apart. The ship then proceeded to occupy stations along the southwest coast of Mindanao with the intention of mapping the coastal circulation. Stations were occupied parallel and perpendicular to the coastline from Moro Gulf to  $7^{\circ}\text{N}$  on the Pacific side of Mindanao (Fig. 29). Most station spacing were 15 nm, near shore to Mindanao.

Both the CTD sampling and processing are similar to that used during the WEPOCS II cruise and are described in the WEPOCS II data report. [Tsuchiya, et al., 1987]. "The data were obtained by a modified Neil Brown Mark III CTD. The CTD data were initially processed into a filtered 1/2 second average time-series during data acquisition. This time series was then pressure-sequenced into 2-decibar pressure intervals. A spike filter was employed to remove large pressure, temperature and conductivity spikes from the time-series data and a "ship-roll" filter was applied to disallow pressure reversals." I will focus my discussion of these data to the thermal structure above 300 m. Vertical profiles, sections, and horizontal charts will be examined to determine the geographic variability and flow patterns.

##### A. VERTICAL PROFILES

The general vertical structure of the region is represented by two CTD profiles (Figs. 30 and 31) selected for comparison at opposite extremes of the survey area. One, near  $7^{\circ}\text{N}$ ,  $127^{\circ}\text{E}$ , station 70, acquired on 16 July, 1988, was in the vicinity of the Mindanao

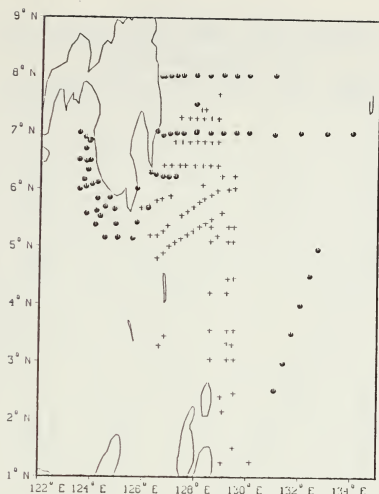


Figure 29. AXBT and CTD Station Locations

Current. The other, Station 32, located near 3°N, 131°E, in the vicinity of the Hahmahera Eddy, was acquired on 8 July, 1988.

The vertical temperature distributions at these stations show a notable difference in the depth and thickness of the thermocline. In the southern waters, the thermocline is located between 100 m and 300 depth, whereas in the northern waters it is located between 30 m and 150 m depth. The salinity maximum represents the Subtropical Lower Waters [Wyrki, 1961]. The northern station has a salinity maximum of 35 ppt and it is located 50 m below the mixed layer at 100 m. The southern station has a slightly higher salinity maximum at 35.2 ppt and is located at 200 m or 100 m below the mixed layer.

## B. VERTICAL SECTIONS

The vertical cross-section plotted at 6.5°N from 127° E to 128.6°E (Fig. 32) , beginning 100 km from the southern coast of Mindanao, shows isotherms generally sloping down toward the coast, consistent with equatorial flow. The greatest slopes are below

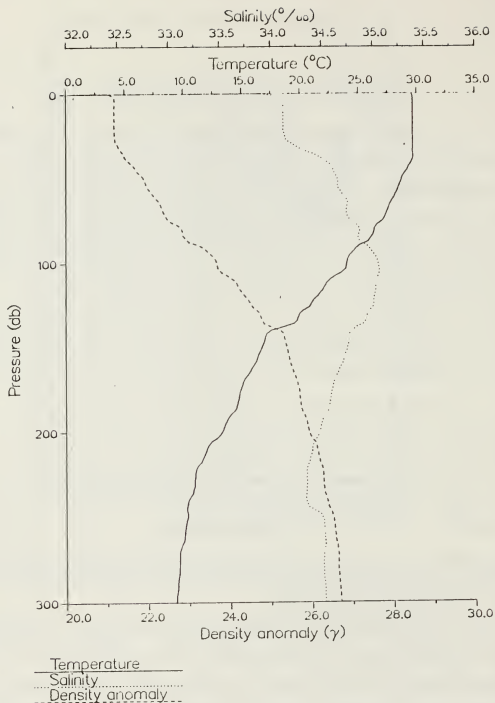


**Figure 30. Vertical Profiles of Temperature, Salinity, and Density Anomaly:** CTD station 70 located at 6.95°N 126.71°E

150 db between 127°E and 127.4°E, and strengthen with depth down to 300 m, which was the limit of the AXBT. Isotherms 22°C-28°C, above 125 m, slope up toward the coast, evidence of possible upwelling. The 10°C-22°C isotherms slope down toward the east at 128.3°E marking the location of the Mindanao eddy. Surface temperatures are about 30°C. Temperatures at 300 db are less than 10°C.



Figure 31. Vertical Profile of Temperature, Salinity, and Density Anomaly: CTD station 32 located at 2.99°N 131.39°E

The north-south cross-section located along 129°E (Fig. 33), and the north-south cross-section located along 130°E (Fig. 34) are through the Halmahera Eddy. Both of these cross-sections have a weaker thermocline gradient than Fig. 32. However, toward the north there is a tightening of the gradient which more closely resembles that found off the coast of Mindanao (Fig. 32). The maximum surface temperature observed in the

two cross-sections is along 129°E and is 30°C. In both cross-sections there is a broad warm core feature between 2.5°N and 5.0°N. It extends to 300 db and the vertical displacement of isotherms is greater with depth. In the western section (Fig. 33) there is a stronger gradient immediately below the mixed layer and a 300 db temperature of less than 12°C south of 3.3°N and greater than 12°C north of 3.3°N. The eastern section (Fig. 34) in addition to having a weaker gradient below the mixed layer, has considerably warmer deep water south of 3.0°N, 14°C and cooler deep water north of 3.8°N, 12°C. Surface temperatures greater than 30°C are formed only close to 5°N at 129°E.

### C. HORIZONTAL TEMPERATURE STRUCTURE

I have chosen two isotherms to characterize the shape of the thermocline in the region, 23°C and 14°C. The 23° isotherm lies close to but below the mixed layer in these data. The 14°C isotherm depth is at the bottom of the thermocline. Its depth exceeded 300 m in a few cases but was measured for all casts.

The depth of the 23°C isotherm (Fig. 35) ranges from 76 m to 169 m. At 8°N the depths increase to the coast (to about 140 m), marking the strong southwest flow of the Mindanao current. The region of shallow depths extends from the Mindanao eddy to the southwest and is outlined by the 110 m contour. In the Halmahera eddy to the southeast, in the area of the SEC, depths are about 130 m. The Mindanao eddy, located at approximately 128.5°N, 7.0°E, is associated with the 23°C isotherm depths shallower than 90 m. To the south, across a frontal boundary which separates the NEC water and SEC water, the Halmahera eddy is located northeast of Halmahera at approximately 129°N, 4°E. Associated with this eddy, the 23°C isotherm deepens to 160 m.

The depth of the 14°C isotherm (Fig. 36) ranges from 135 m to 320 m. Patterns are similar to those of the 23°C isotherm but are better defined and stronger. A 20 m contour interval is used here while a 10 m contour interval is used with the 23°C isotherms. The 160 m contour at 7°N, 128°E marks the location of the Mindanao eddy and is shifted slightly to the southwest of the location at 23°C. At 8°N, the 14°C isotherm deepens to 260 m, so the Mindanao current is strong and clearly delineated. Going to the southwest across the frontal boundary, the 14°C isotherm deepens from 160 m to 240 m. The Halmahera eddy is marked by isotherm depths greater than 300 m.

The depth difference between these two isotherms is a measure of thermocline thickness and is shown in Fig. 37. The differences range from 50 to 20 m.

The geographic distribution seems somewhat bivariate: waters from north of the equator have thicknesses of about 80 m while those from the southern hemisphere have

thicknesses exceeding 120 m. The boundary between these waters is marked by a strong gradient. The location of the Mindanao eddy is best indicated by the closed 60 m contour at 6°N, 128.5°E which is slightly south of the location indicated on the other charts. The eddy off Halmahera is marked by closed contours with thicknesses exceeding 160 m. Fig. 38, a composite of all the buoy trajectories, is included here to show the motion of the buoys relative to the hydrographic features. The Mindanao eddy is delineated east of Mindanao by the cyclonic circulation completed by Buoy 53. Although the Halmahera eddy does not appear on this figure, the anticyclonic recurving pattern across the Philippine Sea is consistent with the presence of a warm core eddy north of Halmahera. The eddy located further to the east at 5°N, 134°E was not resolved with the AXBT data.

#### D. DYNAMIC STRUCTURE

In order to see if the dynamic structure in the region could be calculated from AXBT data, dynamic heights were calculated for the two CTD stations discussed above. First, dynamic height was calculated using the observed salinities and then they were again calculated using a constant salinity of 34.5 ppt. The results are shown in Table 4. From the difference calculations in Table 4 a maximum error of 15% in the dynamic height calculation should be expected when assuming constant salinity. This error was acceptable for further calculations.

Using the CTD data with observed salinities and the AXBT data and an assumed constant salinity of 34.5 ppt, a dynamic height field was calculated for the entire region (Fig. 39). The highest dynamic heights, 1.4 dyn m, are in the region to the south where the thickness is at a maximum. Also, the strong gradient can be seen in this field between the waters from the northern hemisphere and the southern hemisphere. The geostrophic velocity was calculated at this front to be about 70 cm/s, about half the velocity measured by the drifters. In the northern region, dynamic heights are lower, 0.9 to 1.0 dyn m, and the Mindanao eddy does not have a strong signature.

Table 4. DYNAMIC HEIGHT COMPARISONS

Station	Constant Salinity Dynamic Height	Observed Salinity Dynamic Height
32	1.2815	1.259
70	1.0568	.98476
difference	.23	.27

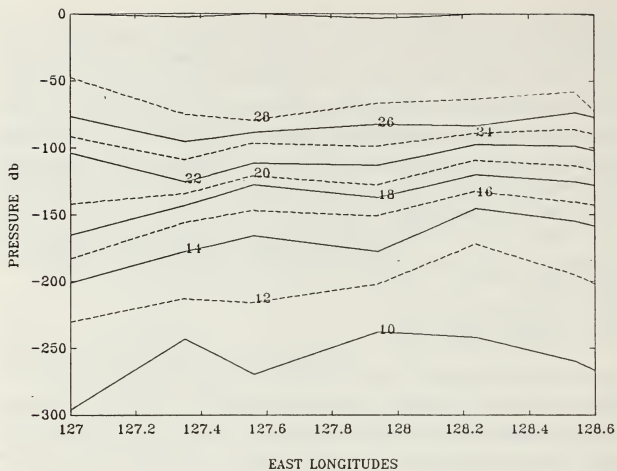


Figure 32. Vertical Temperature Cross-section A: Located along 6.5°N

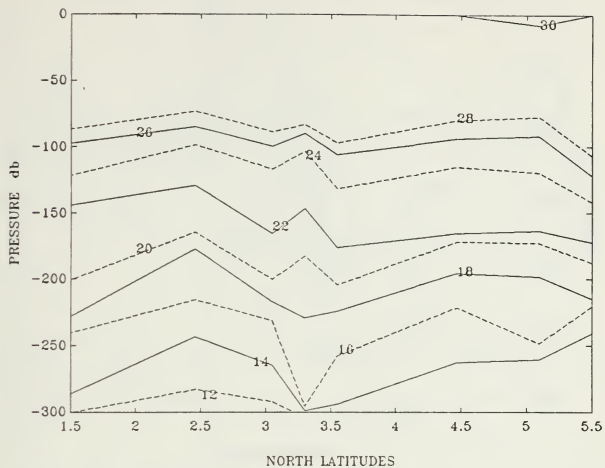


Figure 33. Vertical Temperature Cross-section B: Located along 129°E

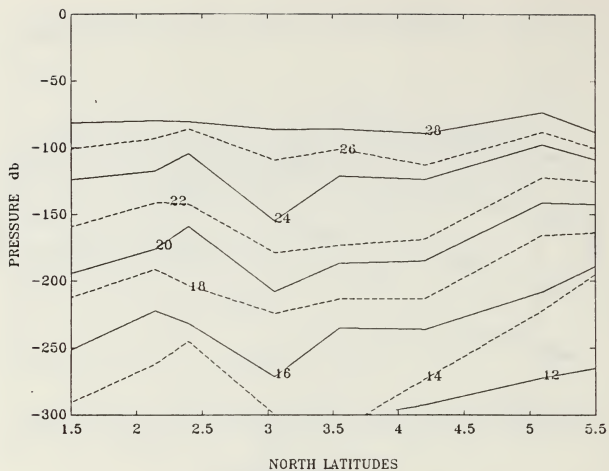


Figure 34. Vertical Temperature Cross-section C: Located along 130°E

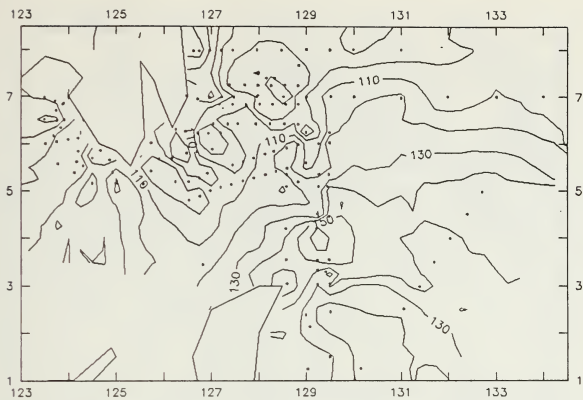


Figure 35. 23° Isotherm

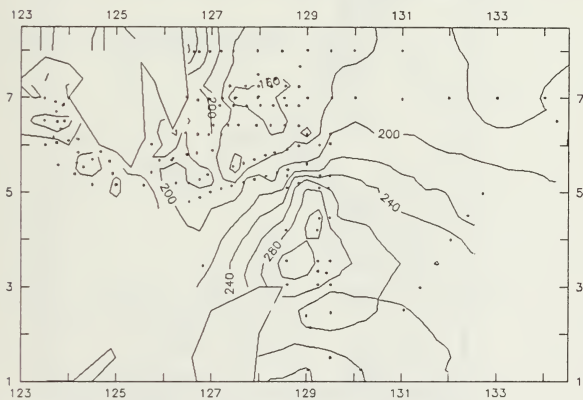


Figure 36. 14° Isotherm

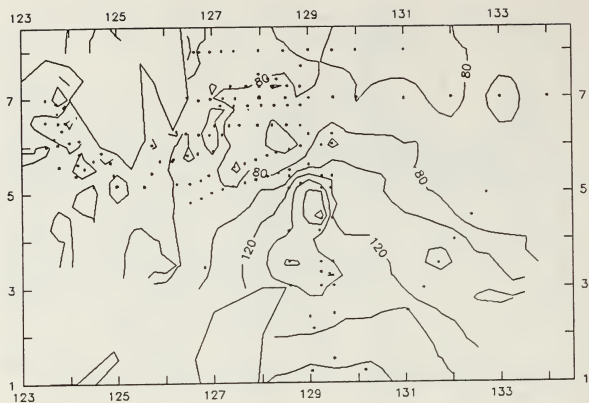


Figure 37. 14°-23° Thickness

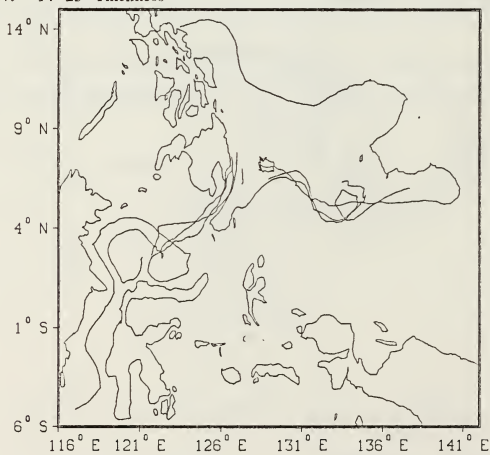


Figure 38. Buoy Trajectory composite

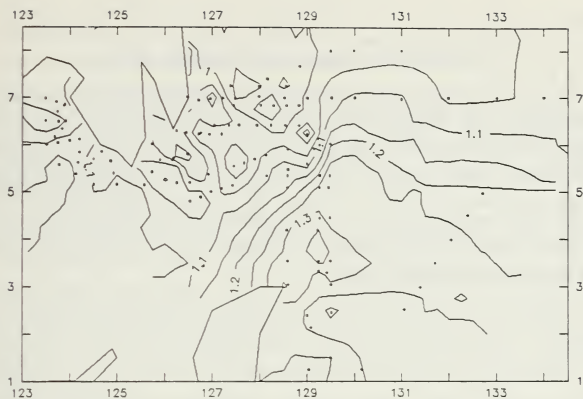


Figure 39. Dynamic Heights 0/300 m

## V. SUMMARY AND RECOMMENDATIONS

Prior to the commencement of TOGA and the subsequent WEPOCS cruises, our understanding of the circulations associated with the western equatorial Pacific and the origin of the NECC had been based upon ship drift reports and widely separated water mass samples. There had been no direct attempt at measuring the current speeds nor had a large scale effort been made to determine the dynamic structure based on closely spaced samples. Hopefully, this study has played a role in closing the gap between the heretofore inference and a true observed description of the circulations associated with the Mindanao and Halmahera Eddies.

The major need for an increased understanding of the circulations in the western equatorial Pacific arises from its link to understanding the global climate (El Nino). The first link to prediction is the climatology of the region of concern. This study should serve as a beginning toward a better understanding of the summertime circulation in the western equatorial Pacific. An understanding of these circulations also has tactical military significance to the United States. The largest forward deployed Naval bases are located in the Philippine Islands and the primary Battle Group Pacific-Indian Ocean transit route is through the western equatorial Pacific and the Indonesian Archipelago. Moreover, every submarine officer knows the importance of being able to predict and locate mesoscale ocean eddies for Anti-Submarine Warfare.

### A. SUMMARY

This study has been an investigation into the circulation associated with the Mindanao and Halmahera eddies in June and July, 1988. The drifter data, as summarized earlier, showed a strong cyclonic shear across the Mindanao current as evidenced by the difference between the maximum velocity on the inshore side of 115 cm/s (Buoy 50) and the minimum velocity on the seaward side of 20 cm/s (Buoy 53). The buoys in the Philippine Sea were observed to interact with three different eddies. The Mindanao Eddy located at 7°N, 128.5°E, the Halmahera Eddy located at 4°N, 129.5°E, and a third unnamed eddy located at 5°N, 133°E. These Eddies mark the origin of the NECC and provide a mechanism for recirculation of water back into the NEC and SEC.

The buoys that drifted into the Celebes Sea were all observed to drift around a large cyclonic gyre that dominated the central Celebes Sea. Buoys 50 and 55 both drifted close to the coast of Borneo and toward the entrance to the Macassar Strait. However, at the

entrance to the Strait Buoy 50 retroflects back to the north and Buoy 55 continues through the Strait. Both buoys experienced an increase in speed along the northeast coast of Borneo. Buoy 50 with the most seaward trajectory accelerated to 80 cm/s and Buoy 55, the inshore trajectory, accelerated to 145 cm/s. These speeds are indicative of a strong narrow current along the northeast coast of Borneo with divergence to the south and north at the entrance to Macassar strait. This indicates a strong cyclonic shear was present across this current in that buoy separation in the Borneo Current was only about 50 km.

From the AXBT survey conducted by the Naval Postgraduate School, the upper ocean temperature structure also shows the horizontal extent of these features. Horizontal depictions of the 23°C and the 14°C isotherms clearly identified the locations of the Mindanao and Halmahera eddies at the time of this survey. The most striking feature observed from these data was the frontal boundary between the SEC water and the NEC water as they retroflect then converge to form the origin of the NECC. Drifter speeds in excess of 120 cm/s were observed in this region at approximately 5°N, 128.5°E (Buoy 52).

## **B. RECOMMENDATIONS**

Any conclusions drawn from this study have limited scope and must be supplemented with additional research. In this study there has been no correlation attempted between the buoy trajectories and the synoptic weather that occurred in June and July, 1988. This needs to be done. The seasonal evolution of the circulations associated with these eddies can only be inferred until this study is repeated during the northwest monsoon season.

The Pacific-Indian Ocean throughflow is a stated objective of TOGA and WEPOCS. This study provided a glimpse of this throughflow via the trajectory of Buoy 55. However, this is only a sample size of one. I highly recommend that any subsequent cruises to this region be extended to include a more thorough investigation of the mechanisms for the transport of north Pacific water to the Indian Ocean.

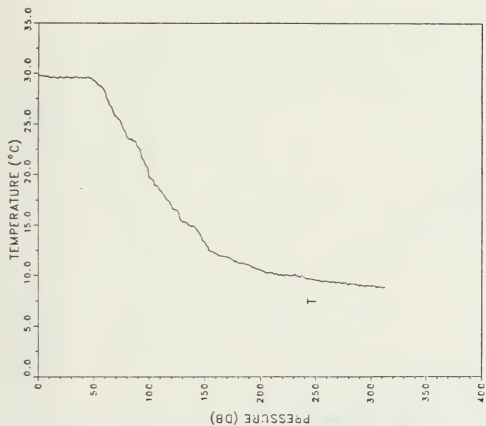
## APPENDIX A. AXBT TEMPERATURE PROFILES

Data collection in support of the ONR sponsored Eddy Study occurred on the evenings of 11, 12, and 13 July 1988. Over the course of 33.2 air hours logged, 133 Airborne Expendable Bathythermographs (AXBTs) were deployed, using channels 12, 14 and 16. Reserve squadron VP-69 (from Whidby Island, WA) assets at NAS Cubi Point, RP provided the P-3 platform, as well as significant technical and logistical support. Additional coordination and support was provided by VP-17 and the Naval Oceanography Command Facility at NAS Cubi Point.

The intended collection procedure was to install an Airborne Digital Data Acquisition System (ADDAS) on board the P-3 and digitally record and perform in situ analyses of AXBT measurements. The ADDAS was misrouted in shipping and did not arrive at NAS Cubi Point in time for scheduled use, precluding its use in the actual collection process. The data was recorded via on board BT profile output strip charts, anograms, and magnetic tape to be later transcribed on VHS tape using the ADDAS at the Cubi Point ASWOC, and post-processed at the Naval Postgraduate School.

During collection, the average on station altitude was 2,500 feet and the average ground speed was 225 knots. There was approximately a 28% failure rate either due to AXBTs not "lighting off", sending a weak signal, or due to a recording failure on board the aircraft.

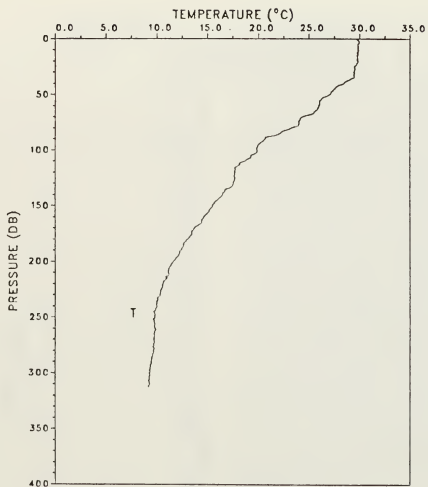
Included in this appendix are vertical profiles and listings of temperature at standard depths. The Longitudes given are east.



PRESS	TEMP
1	29.805
11	29.570
21	29.593
31	29.610
40	29.620
50	29.320
75	24.973
101	19.610
125	16.440
150	13.300
176	11.470
200	10.540
225	10.045
251	9.550
275	9.300
300	9.050
313	8.800

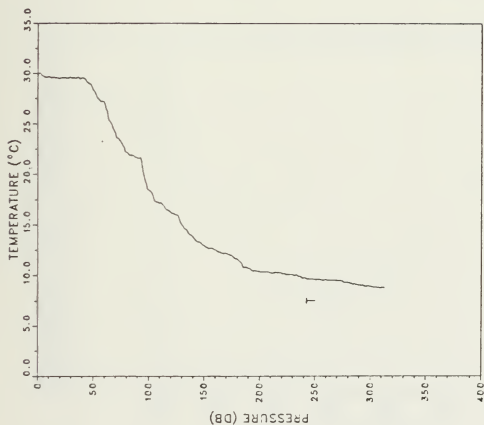
STATION: 4  
 LAT: 7 23.6 N  
 DATE: 7/12/88

LON: 128 9.7  
 TIME: 1106Z



PRESS	TEMP
1	29.760
11	29.823
21	29.853
31	29.495
40	28.405
50	27.075
75	23.990
101	19.867
125	17.680
150	15.510
176	13.507
200	11.620
225	10.385
251	9.757
275	9.710
300	9.260
313	9.160

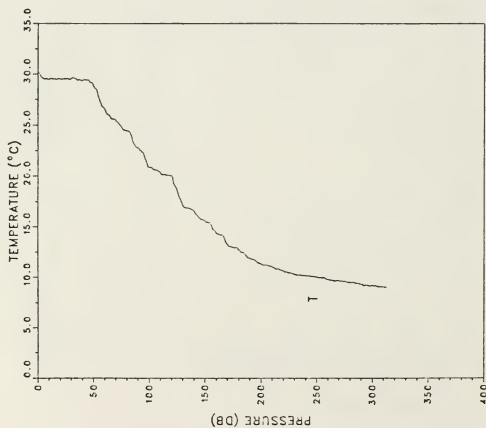
STATION: 6 LAT: 7 39.8 N LON: 128 50.9  
 DATE: 7/12/88 TIME: 1118Z



PRESS	TEMP
1	29.970
11	29.610
21	29.573
31	29.555
40	29.560
50	28.400
75	23.250
101	18.400
125	15.965
150	12.930
176	11.883
200	10.370
225	10.120
251	9.607
275	9.440
300	8.945
313	8.790

STATION: 8    LAT: 7    14.9 N    LON: 128    32.9  
 DATE: 7/12/88    TIME: 1130Z

PRESS	TEMP
1	30.125
11	29.570
21	29.507
31	29.655
40	29.380
50	28.885
75	24.873
101	20.863
125	18.630
150	15.500
176	12.897
200	11.330
225	10.440
251	9.970
275	9.615
300	9.190
313	9.030

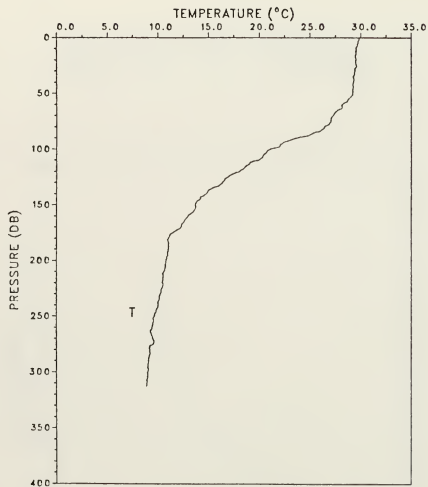


STATION: 10    LAT: 7    14.4 N    LON: 127    58.9  
 DATE: 7/12/88    TIME: 1141Z

PRESS	TEMP
1	29.885
11	29.403
21	29.337
31	29.310
40	29.085
50	28.845
75	27.417
101	23.780
125	21.195
150	16.260
176	13.563
200	12.505
225	12.180
251	10.830
275	10.535
300	9.815
313	9.660

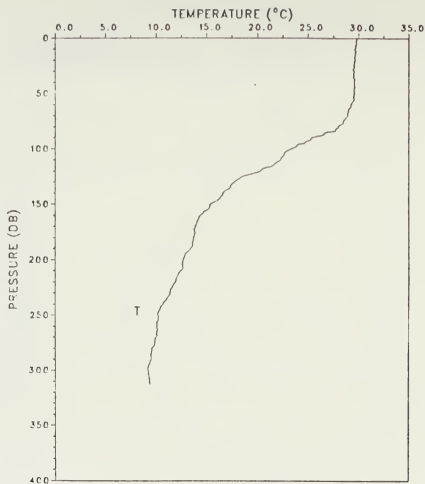


STATION: 12    LAT: 7    15.1 N    LON: 127    22.9  
 DATE: 7/12/88    TIME: 1153Z



PRESS	TEMP
1	29.850
11	29.567
21	29.503
31	29.380
40	29.290
50	29.195
75	27.053
101	20.907
125	16.905
150	13.720
176	11.280
200	10.780
225	10.355
251	9.563
275	9.535
300	9.005
313	8.860

STATION: 14 LAT: 6 49.8 N LON: 127 27.0  
 DATE: 7/12/88 TIME: 1211Z



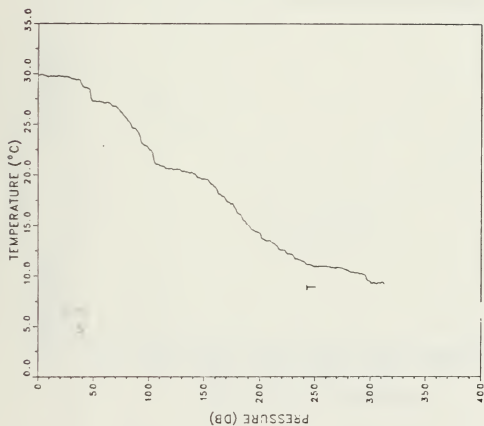
PRESS	TEMP
1	29.775
11	29.677
21	29.567
31	29.550
40	29.580
50	29.540
75	28.453
101	23.110
125	18.475
150	15.340
176	13.793
200	12.685
225	11.535
251	10.203
275	9.850
300	9.190
313	9.370

STATION: 16 LAT: 6 50.4 N LON: 128 1.0  
 DATE: 7/12/88 TIME: 1236Z



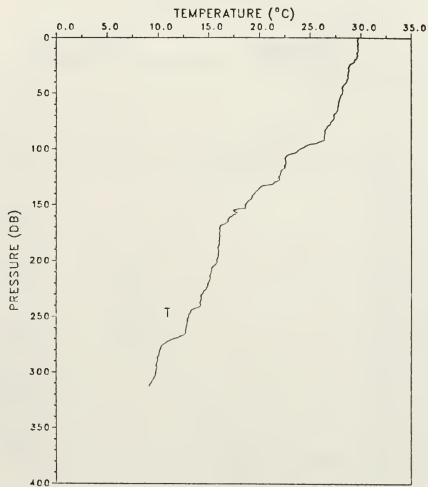
PRESS	TEMP
1	30.135
11	29.613
21	29.627
31	29.710
40	29.620
50	29.630
75	27.967
101	25.093
125	22.250
150	17.345
176	14.037
200	12.260
225	10.980
251	9.743
275	9.360
300	9.285
313	8.820

STATION: T LAI: 6 50.2 N  
 DATE: 7/12/88  
 LONG: 128 17.5  
 TIME: 1236Z



PRESS	TEMP
1	29.850
11	29.787
21	29.760
31	29.495
40	28.860
50	27.315
75	26.200
101	22.453
125	20.580
150	19.640
176	17.143
200	14.225
225	12.165
251	10.993
275	10.740
300	9.415
313	9.210

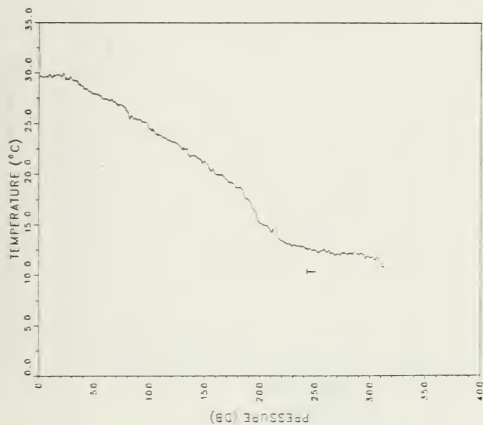
STATION: 18 LAT: 6 50.0 N LON: 128 34.0 W  
 DATE: 7/12/88 TIME: 1241Z



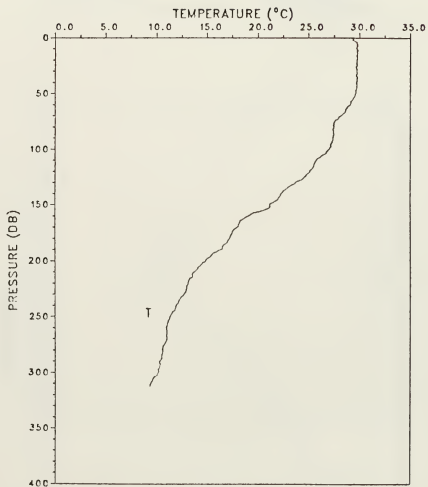
PRESS TEMP

1	29.745
11	29.737
21	29.363
31	28.755
40	28.570
50	28.215
75	27.127
101	23.913
125	21.915
150	18.605
176	16.057
200	15.785
225	14.720
251	13.017
275	10.545
300	9.785
313	9.180

STATION: 19 LAT: 6 50.0 N LON: 0 0.0  
 DATE: 7/12/88 TIME: 1248Z

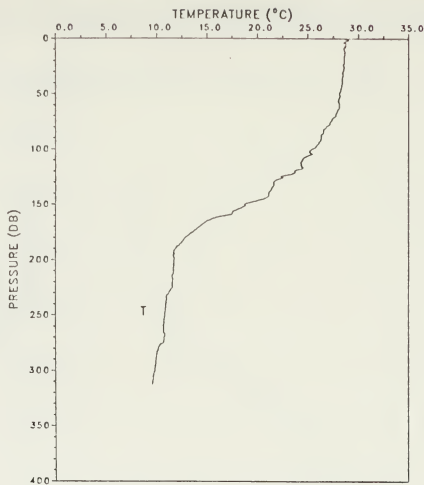


STATION: 20 LAT: 6 24.8 N  
 DATE: 7/12/88  
 LONG: 128 49.9 E  
 TIME: 1253Z



PRESS	TEMP
1	29.350
11	29.830
21	29.747
31	29.760
40	29.685
50	29.560
75	27.523
101	26.860
125	24.545
150	21.155
176	17.450
200	14.840
225	12.930
251	11.273
275	10.755
300	10.130
313	9.340

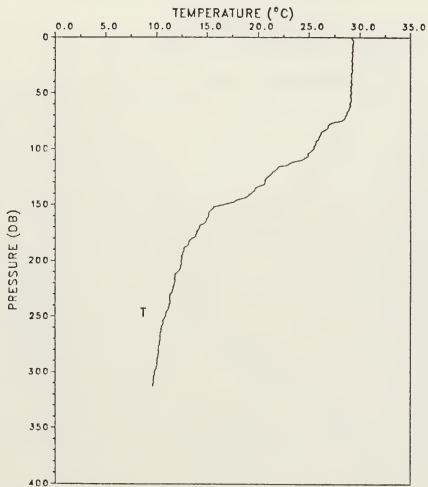
STATION: 21 LAT: 6 25.0 N LON: 128 32.4  
 DATE: 7/12/88 TIME: 1300Z



PRESS TEMP

1	28.775
11	28.607
21	28.607
31	28.400
40	28.420
50	28.105
75	27.250
101	25.293
125	22.310
150	18.735
176	13.407
200	11.670
225	11.500
251	10.763
275	10.660
300	9.785
313	9.550

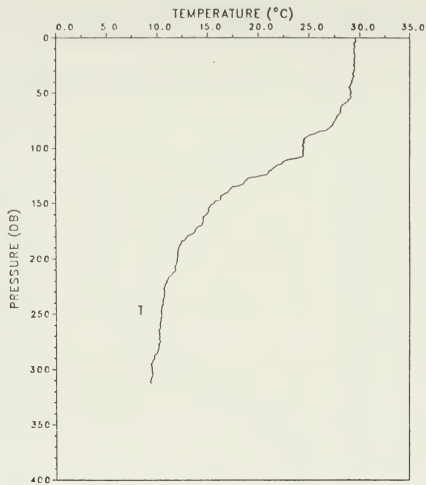
STATION: 22 LAT: 6 25.1 N LON: 128 14.5  
 DATE: 7/12/88 TIME: 1306Z



PRESS TEMP

1	29.210
11	29.307
21	29.193
31	29.280
40	29.140
50	29.180
75	28.197
101	25.377
125	20.990
150	16.480
176	13.877
200	12.375
225	11.565
251	10.753
275	10.265
300	9.760
313	9.640

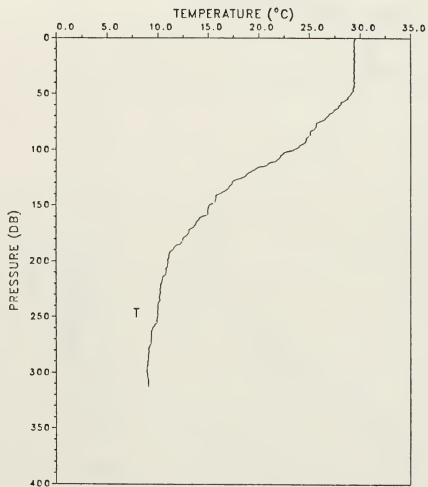
STATION: 23 LAT: 6 25.1 N LON: 127 56.2  
 DATE: 7/12/88 TIME: 1311Z



PRESS TEMP

1	29.600
11	29.470
21	29.487
31	29.450
40	29.225
50	29.145
75	27.567
101	24.447
125	20.380
150	15.595
176	13.707
200	11.990
225	10.745
251	10.437
275	10.350
300	9.480
313	9.360

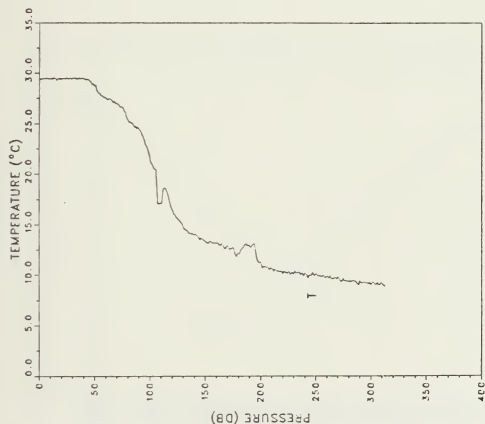
STATION: 24 LAT: 6 25.2 N LON: 127 33.5 W  
 DATE: 7/12/88 TIME: 1318Z



PRESS TEMP

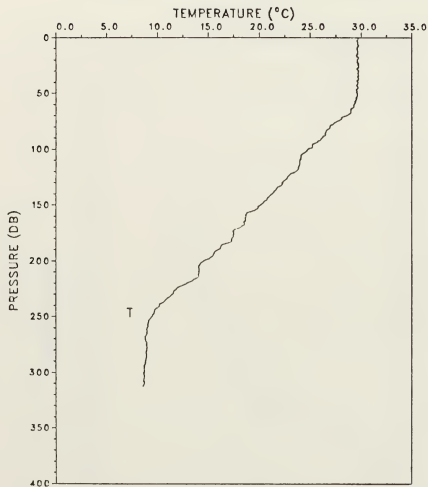
1	29.480
11	29.377
21	29.467
31	29.375
40	29.485
50	29.110
75	26.000
101	23.340
125	18.490
150	15.045
176	12.887
200	10.995
225	10.205
251	9.977
275	9.250
300	8.990
313	9.080

STATION: 25 LAT: 6 25.1 N LON: 127 20.9 W  
 DATE: 7/12/88 TIME: 1323Z



PRESS	TEMP
1	29.415
11	29.487
21	29.457
31	29.515
40	29.460
50	28.780
75	26.637
101	21.203
125	15.625
150	13.305
176	12.627
200	11.305
225	10.310
251	10.017
275	9.655
300	9.015
313	8.860

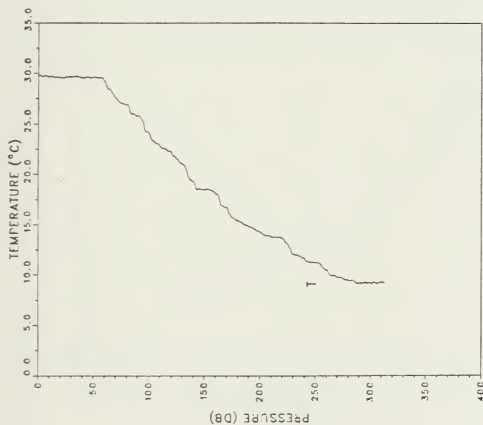
STATION: 26 LAT: 6 25.0 N LON: 0 0.0  
DATE: 7/12/88 TIME: 1330Z



PRESS TEMP

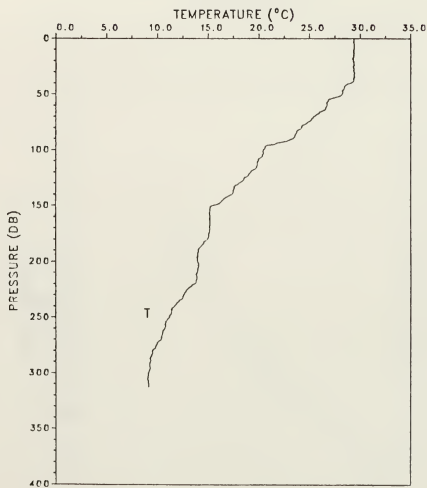
1	29.705
11	29.620
21	29.620
31	29.725
40	29.715
50	29.630
75	27.697
101	24.690
125	22.750
150	20.080
176	17.470
200	14.535
225	11.825
251	9.353
275	8.910
300	8.650
313	8.560

STATION: 28 LAT: 5 40.5 N LON: 125 54.1  
DATE: 7/12/88 TIME: 1353Z



PRESS	TEMP
1	29.855
11	29.693
21	29.640
31	29.685
40	29.550
50	29.675
75	27.057
101	23.890
125	21.495
150	18.435
176	15.623
200	14.240
225	13.005
251	11.163
275	9.605
300	9.265
313	9.180

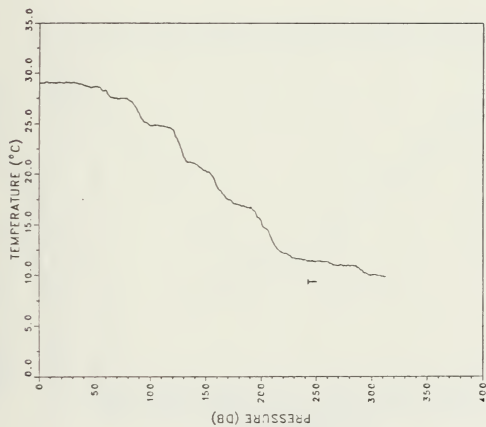
STATION: 29 LAT: 5 43.4 N  
 DATE: 7/12/88  
 LON: 126 11.7  
 TIME: 1400Z



PRESS TEMP

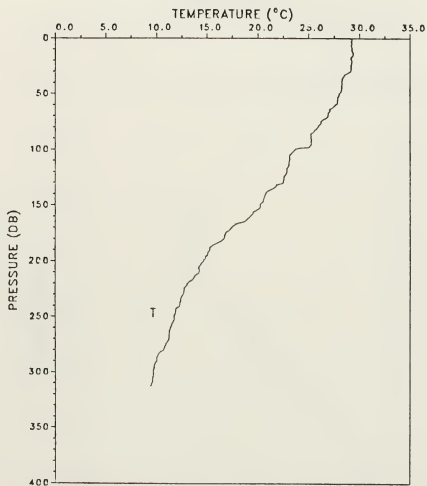
1	29.380
11	29.360
21	29.357
31	29.445
40	29.050
50	28.195
75	24.800
101	20.397
125	18.550
150	15.325
176	15.030
200	13.970
225	12.875
251	11.073
275	9.870
300	9.120
313	9.160

STATION: 30 LAT: 5 48.1 N LON: 126 29.1 .  
DATE: 7/12/88 TIME: 1406Z



STATION: 42 LAT: 5 46.8 N  
 DATE: 7/12/88

LON: 128 7.7  
 TIME: 1518Z

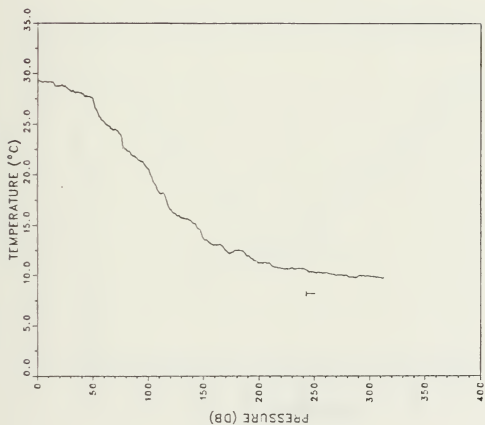


PRESS TEMP

1	29.230
11	29.263
21	29.233
31	28.990
40	28.310
50	27.980
75	26.187
101	23.567
125	22.535
150	20.220
176	16.767
200	14.620
225	12.700
251	11.747
275	10.905
300	9.680
313	9.460

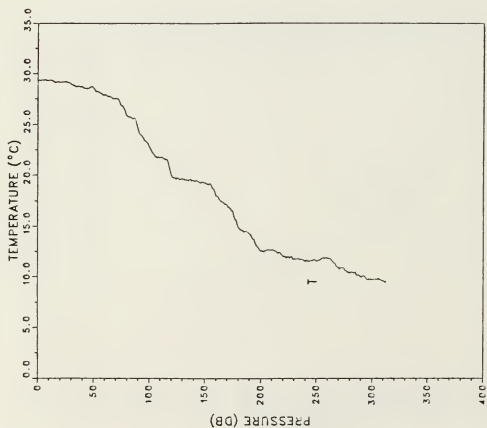
STATION: 43 LAT: 5 41.7 N LON: 127 54.2  
 DATE: 7/12/88 TIME: 1530Z

PRESS	TEMP
1	29.305
11	29.200
21	28.807
31	28.215
40	27.995
50	27.505
75	23.990
101	20.447
125	16.130
150	13.625
176	12.290
200	11.230
225	10.555
251	10.250
275	10.020
300	9.890
313	9.770

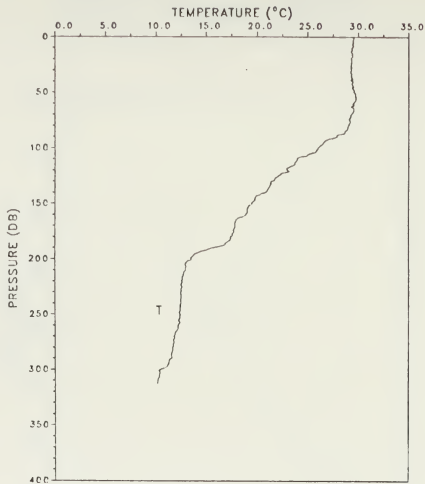


STATION: 90 LAT: 6 13.9 N  
 DATE: 7/11/98  
 LON: 129 0.2 W  
 TIME: 0853Z

PRESS	TEMP
1	29.365
11	29.377
21	29.170
31	28.900
40	28.705
50	28.600
75	26.853
101	22.660
125	19.720
150	19.275
176	16.040
200	12.510
225	11.905
251	11.583
275	10.805
300	9.685
313	9.520

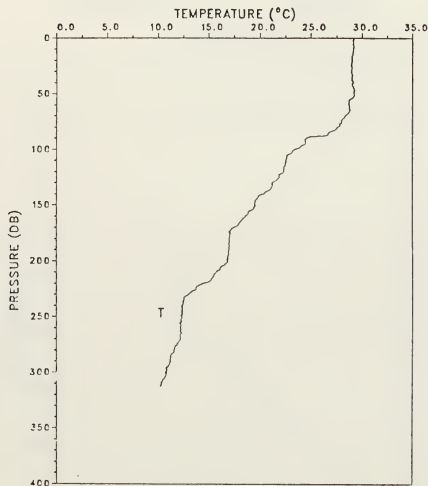


STATION: 91 LAT: 5 35.7 N  
 DATE: 7/11/88  
 LON: 129 0.1  
 TIME: 0911Z



PRESS	TEMP
1	29.525
11	29.343
21	29.317
31	29.235
40	29.445
50	29.550
75	29.173
101	25.957
125	22.090
150	19.445
176	17.663
200	13.470
225	12.580
251	12.353
275	11.760
300	10.420
313	10.140

STATION: 92 LAT: 5 21.0 N LON: 128 35.5  
 DATE: 7/11/88 TIME: 0918Z

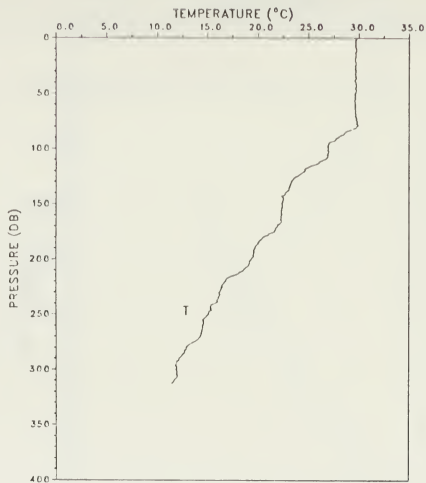


PRESS TEMP

1	29.180
11	29.140
21	29.040
31	28.980
40	29.110
50	29.255
75	27.983
101	23.263
125	21.895
150	19.540
176	17.070
200	16.835
225	13.700
251	12.343
275	11.905
300	10.705
313	10.290

STATION: 93 LAT: 5 5.8 N  
DATE: 7/11/88

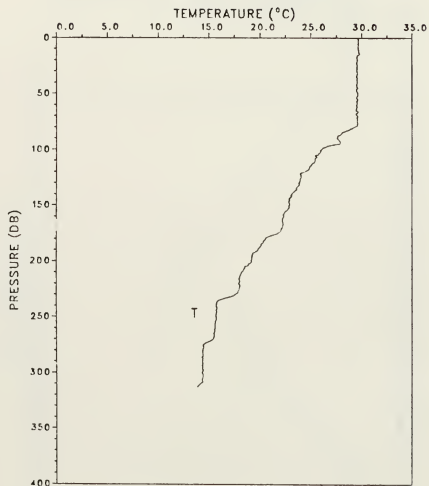
LON: 128 34.9  
TIME: 0923Z



PRESS TEMP

1	29.785
11	29.747
21	29.623
31	29.660
40	29.715
50	29.625
75	29.827
101	26.930
125	23.900
150	22.400
176	21.417
200	19.330
225	16.490
251	14.970
275	13.625
300	11.875
313	11.450

STATION: 95 LAT: 4 12.0 N LON: 128 34.4 W  
 DATE: 7/11/88 TIME: 0936Z

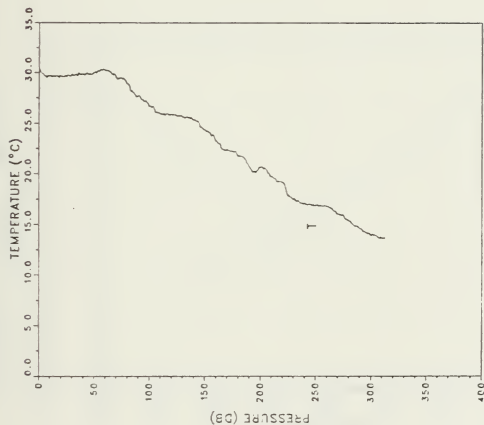


PRESS	TEMP
1	29.650
11	29.717
21	29.590
31	29.590
40	29.570
50	29.620
75	29.590
101	25.993
125	24.030
150	22.850
176	21.563
200	19.160
225	17.955
251	15.660
275	14.440
300	14.330
313	13.860

STATION: 96 LAT: 3 33.0 N LON: 128 34.9 "

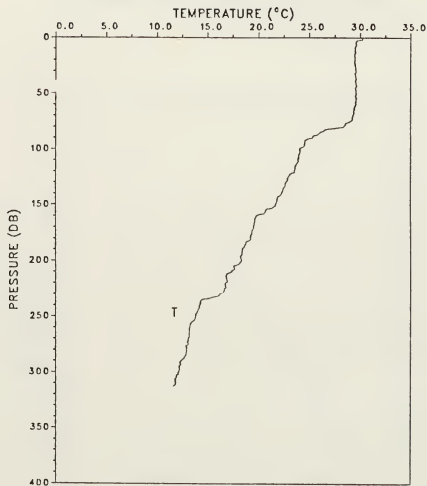
DATE: 7/11/88

TIME: 0948Z



STATION: 9B LAT: 3 2.8 N  
 DATE: 7/11/88

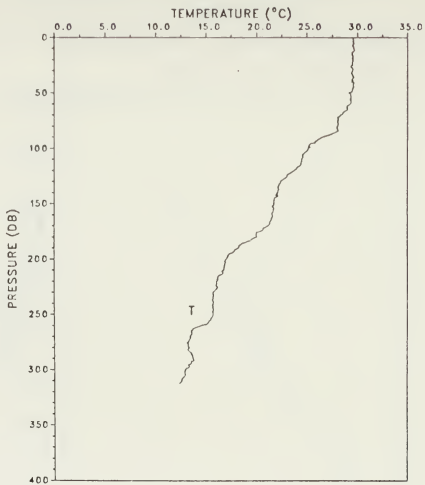
LON: 128 35.8  
 TIME: 0953Z



PRESS TEMP

1	30.235
11	29.487
21	29.447
31	29.565
40	29.565
50	29.640
75	29.003
101	24.107
125	22.910
150	21.650
176	19.360
200	18.280
225	16.640
251	13.797
275	13.105
300	12.110
313	11.620

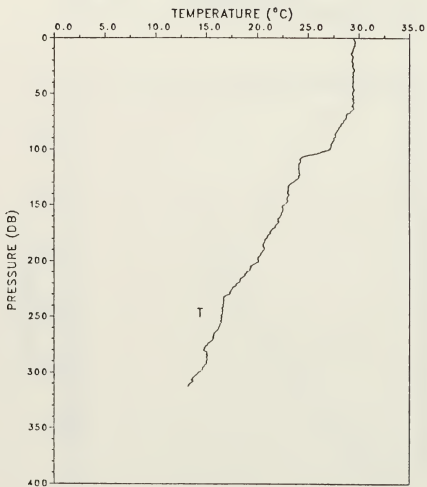
STATION: 99 LAT: 2 23.6 N LON: 129 0.2  
 DATE: 7/11/88 TIME: 1000Z



PRESS TEMP

1	29.595
11	29.697
21	29.550
31	29.500
40	29.390
50	29.170
75	28.013
101	25.113
125	23.005
150	21.720
176	19.963
200	16.950
225	16.200
251	15.640
275	13.245
300	12.920
313	12.350

STATION: 100 LAT: 2 8.5 N LON: 129 4.8  
DATE: 7/11/88 TIME: 1011Z

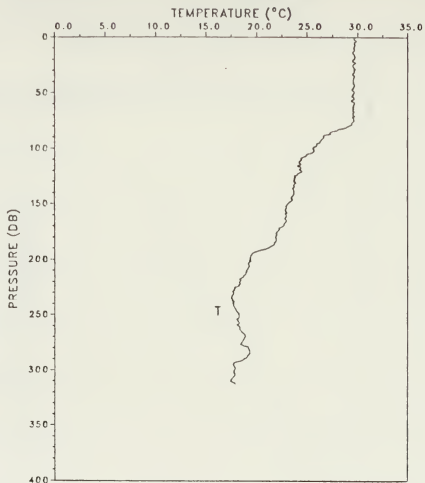


PRESS TEMP

1	29.505
11	29.443
21	29.297
31	29.415
40	29.385
50	29.380
75	28.520
101	26.910
125	24.085
150	22.555
176	21.200
200	20.120
225	17.510
251	16.470
275	15.105
300	14.185
313	13.170

STATION: 102 LAT: 1 14.8 N  
DATE: 7/11/88

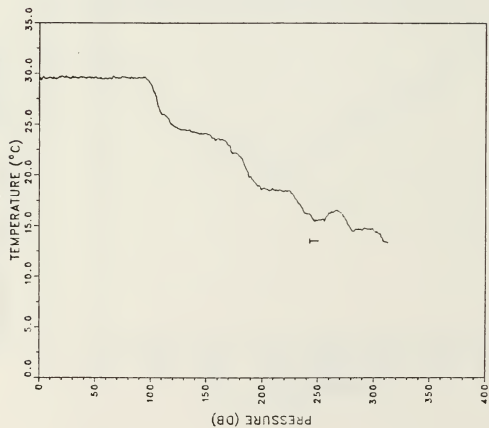
LON: 129 2.5 W  
TIME: 1023Z



PRESS TEMP

1	29.650
11	29.693
21	29.513
31	29.665
40	29.570
50	29.650
75	29.680
101	25.657
125	23.725
150	23.045
176	21.930
200	19.405
225	17.835
251	18.250
275	18.515
300	17.775
313	17.860

STATION: 108 LAT: 3 20.0 N LON: 129 14.5  
 DATE: 7/11/88 TIME: 1053Z

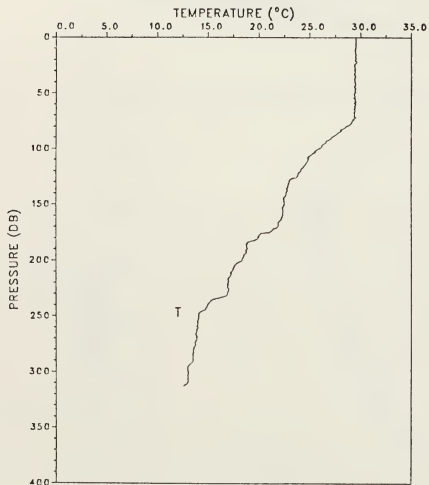


STATION: 109 LAT: 3 32.8 N  
 DATE: 7/11/88  
 LON: 129 14.6  
 TIME: 1106Z

PRESS	TEMP
1	29.830
11	29.773
21	29.340
31	29.720
40	29.645
50	29.760
75	27.637
101	24.357
125	22.835
150	21.915
176	20.870
200	19.485
225	19.220
251	18.700
275	17.680
300	16.610
313	16.870



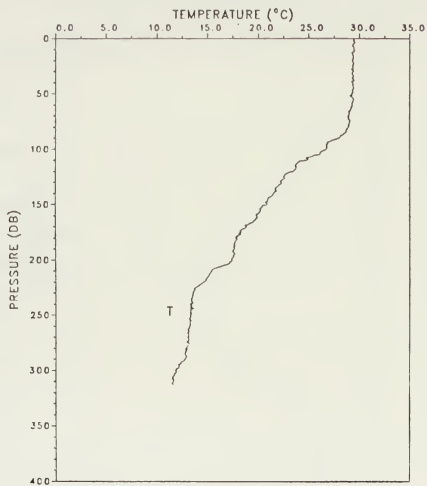
STATION: 110 LAT: 4 12.1 N  
 DATE: 7/11/88  
 LONG: 129 13.5  
 TIME: 1111Z



PRESS TEMP

1	29.545
11	29.453
21	29.467
31	29.480
40	29.415
50	29.405
75	29.163
101	25.740
125	23.765
150	22.395
176	20.170
200	18.330
225	17.005
251	14.100
275	13.745
300	12.970
313	12.590

STATION: 111 LAT: 4 27.1 N LON: 129 15.7  
 DATE: 7/11/88 TIME: 1118Z

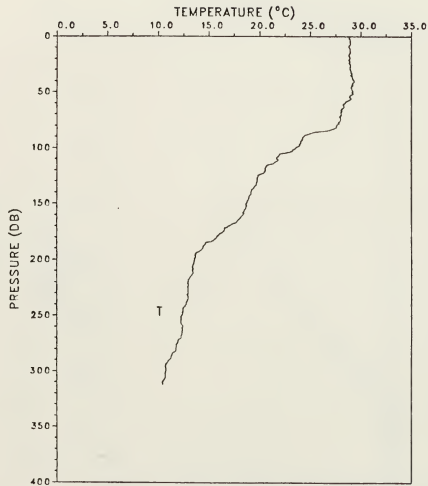


PRESS TEMP

1	29.470
11	29.540
21	29.353
31	29.295
40	29.325
50	29.235
75	29.010
101	26.557
125	22.450
150	20.805
176	18.073
200	17.400
225	13.800
251	13.333
275	13.115
300	11.805
313	11.580

STATION: 112 LAT: 5 5.8 N  
DATE: 7/11/88

LON: 129 15.8  
TIME: 1123Z

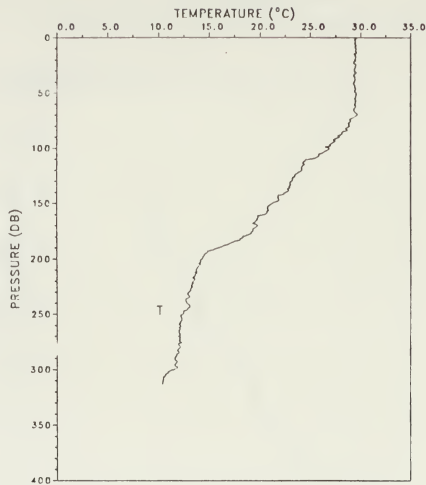


PRESS TEMP

1	28.830
11	28.923
21	28.807
31	29.015
40	29.370
50	29.170
75	27.977
101	23.480
125	19.830
150	18.640
176	16.323
200	13.570
225	12.945
251	12.210
275	11.855
300	10.740
313	10.450

STATION: 113 LAT: 5 21.0 N  
DATE: 7/1/88

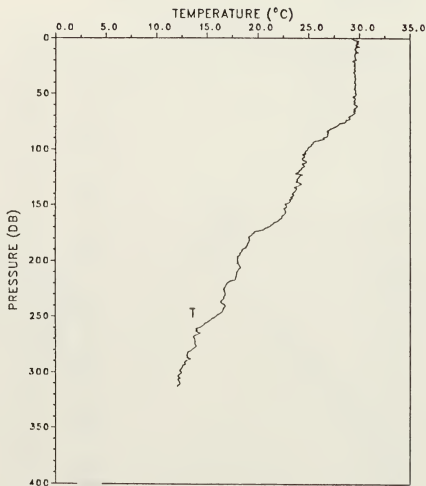
LON: 129 16.3 W  
TIME: 1130Z



PRESS	TEMP
1	29.615
11	29.493
21	29.490
31	29.355
40	29.390
50	29.520
75	28.967
101	26.863
125	23.445
150	21.180
176	19.133
200	14.245
225	13.350
251	12.183
275	12.130
300	11.490
313	10.370

STATION: 114 LAT: 6 0.1 N  
DATE: 7/11/88

LON: 129 15.8  
TIME: 1136Z

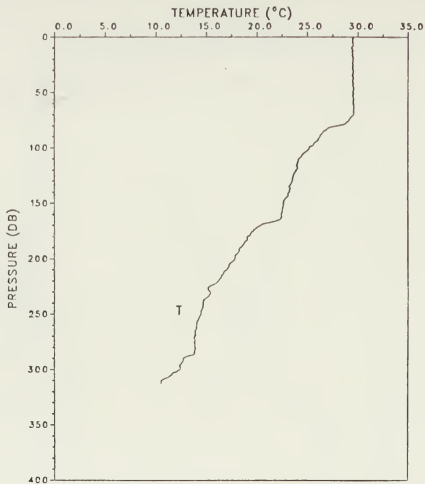


PRESS TEMP

1	29.285
11	29.673
21	29.310
31	29.420
40	29.505
50	29.675
75	28.667
101	24.817
125	24.030
150	22.810
176	19.403
200	18.015
225	16.640
251	15.617
275	13.775
300	12.445
313	12.050

STATION: 117 LAT: 6 1.6 N  
DATE: 7/11/88

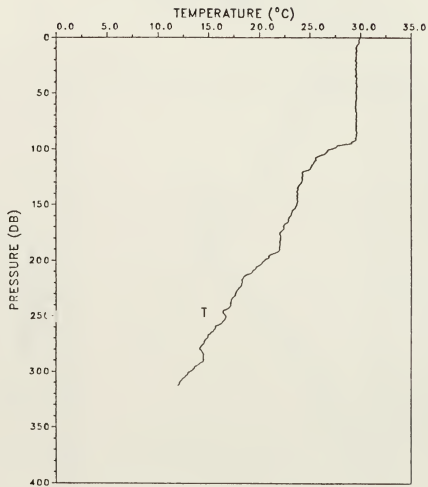
LON: 129 29.5 ✓  
TIME: 1148Z



PRESS TEMP

1	29.565
11	29.437
21	29.517
31	29.525
40	29.505
50	29.535
75	29.100
101	25.173
125	23.630
150	22.700
176	19.457
200	17.810
225	15.270
251	14.380
275	13.810
300	12.375
313	10.480

STATION: 118 LAT: 5 21.0 N LON: 129 29.1 W  
 DATE: 7/11/88 TIME: 1200Z

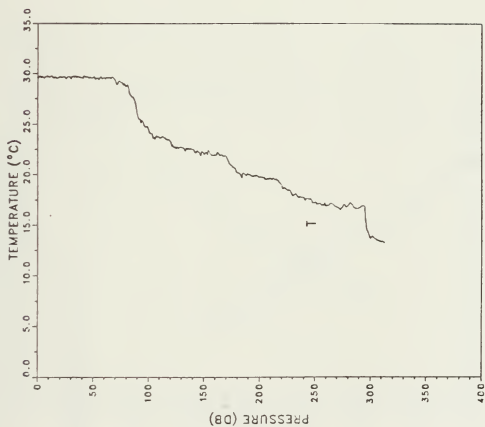


PRESS	TEMP
1	29.940
11	29.607
21	29.457
31	29.580
40	29.585
50	29.585
75	29.573
101	26.733
125	24.215
150	23.700
176	22.000
200	20.475
225	17.920
251	16.663
275	14.510
300	13.210
313	11.970

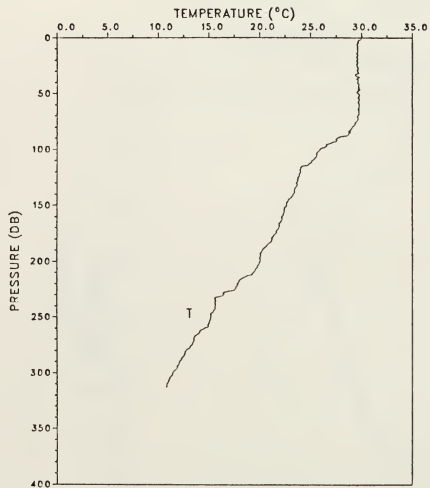
STATION: 119 LAT: 5 5.8 N  
DATE: 7/11/88

LON: 129 27.1  
TIME: 1206Z

PRESS	TEMP
1	29.615
11	29.677
21	29.617
31	29.705
40	29.605
50	29.600
75	29.093
101	24.127
125	22.605
150	21.975
176	20.757
200	19.740
225	18.435
251	17.207
275	16.760
300	13.645
313	13.240



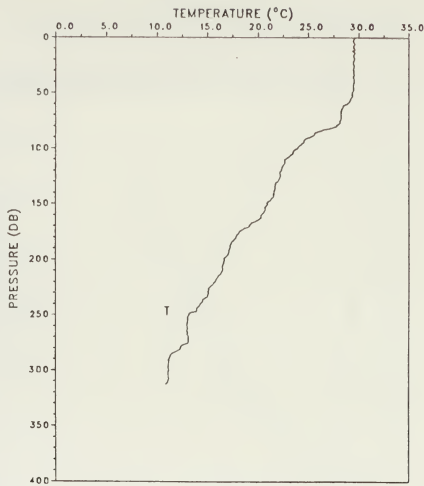
STATION: 120 LAT: 4 27.8 N LON: 129 29.0  
DATE: 7/11/88 TIME: 1211Z



PRESS TEMP

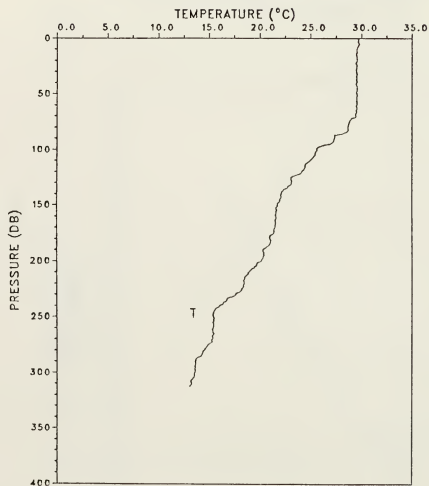
1	29.960
11	29.617
21	29.510
31	29.675
40	29.625
50	29.615
75	29.500
101	25.857
125	23.745
150	22.615
176	21.467
200	20.020
225	17.525
251	15.160
275	13.320
300	11.390
313	10.770

STATION: 122 LAT: 3 33.0 N LON: 129 29.5  
 DATE: 97/11/88 TIME: 1223Z



PRESS	TEMP
1	29.610
11	29.610
21	29.497
31	29.485
40	29.490
50	29.375
75	28.140
101	23.697
125	22.180
150	20.950
176	18.070
200	16.660
225	15.175
251	13.060
275	13.100
300	11.160
313	10.840

STATION: 123 LAT: 3 18.0 N LON: 129 25.4  
 DATE: 7/11/88 TIME: 1230Z



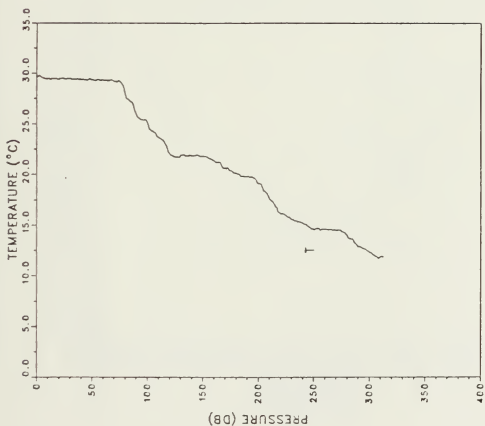
PRESS TEMP

1	29.705
11	29.550
21	29.523
31	29.540
40	29.510
50	29.560
75	28.807
101	25.577
125	23.055
150	21.765
176	21.243
200	20.080
225	18.185
251	15.503
275	14.880
300	13.540
313	13.060

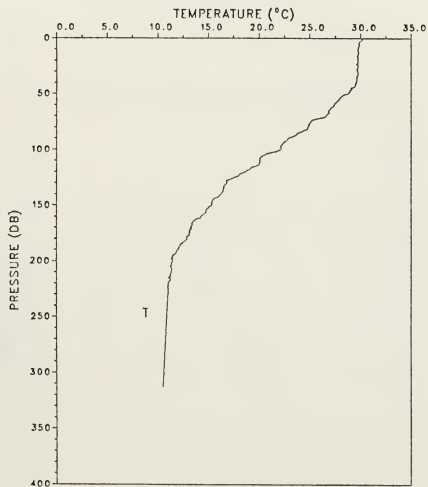
STATION: 124 LAT: 3 2.8 N  
DATE: 7/11/88

LON: 129 30.0  
TIME: 1241Z

PRESS	TEMP
1	29.685
11	29.490
21	29.507
31	29.440
40	29.385
50	29.390
75	29.213
101	24.857
125	21.710
150	21.785
176	20.350
200	19.115
225	15.920
251	14.630
275	14.405
300	12.325
313	11.900



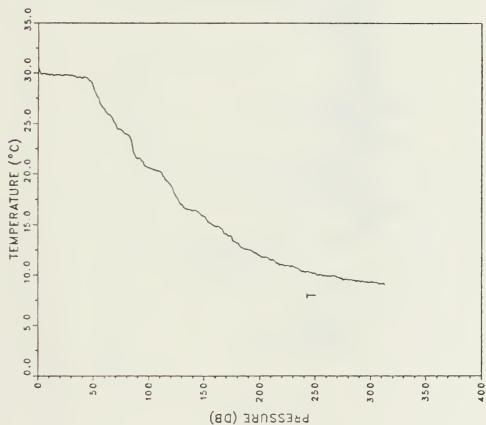
STATION: 126 LAT: 2 27.4 N  
 DATE: 7/11/88



PRESS TEMP

1	30.120
11	29.743
21	29.757
31	29.770
40	29.580
50	28.745
75	25.063
101	21.943
125	17.615
150	15.285
176	13.057
200	11.445
225	11.010
251	10.860
275	10.720
300	10.570
313	10.500

STATION: 127 LAT: 1 30.4 N LON: 129 30.0  
DATE: 7/11/88 TIME: 1253Z

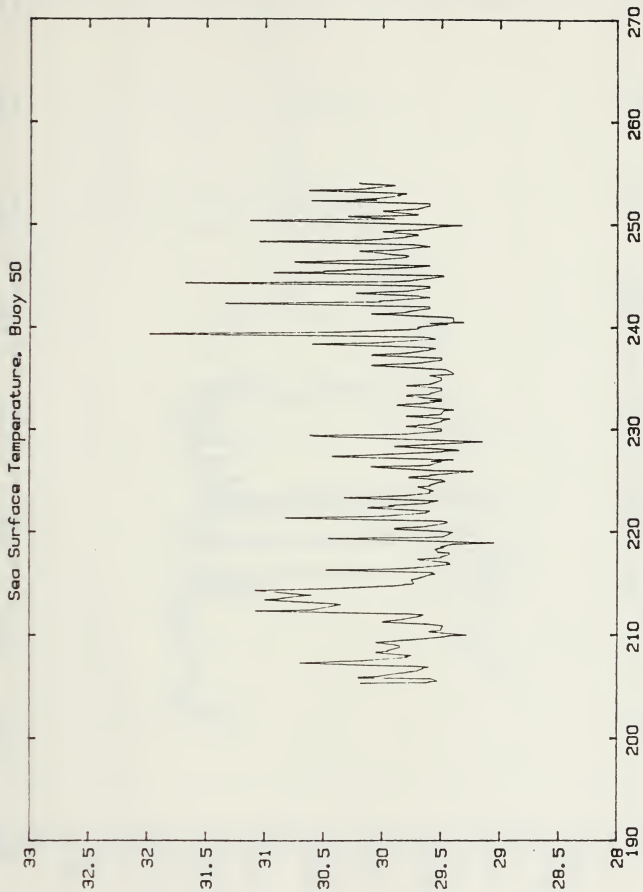


PRESS	TEMP
1	30.450
11	29.883
21	29.750
31	29.760
40	29.515
50	28.575
75	24.337
101	20.553
125	17.745
150	15.810
176	13.400
200	11.925
225	10.920
251	10.047
275	9.565
300	9.345
313	9.010

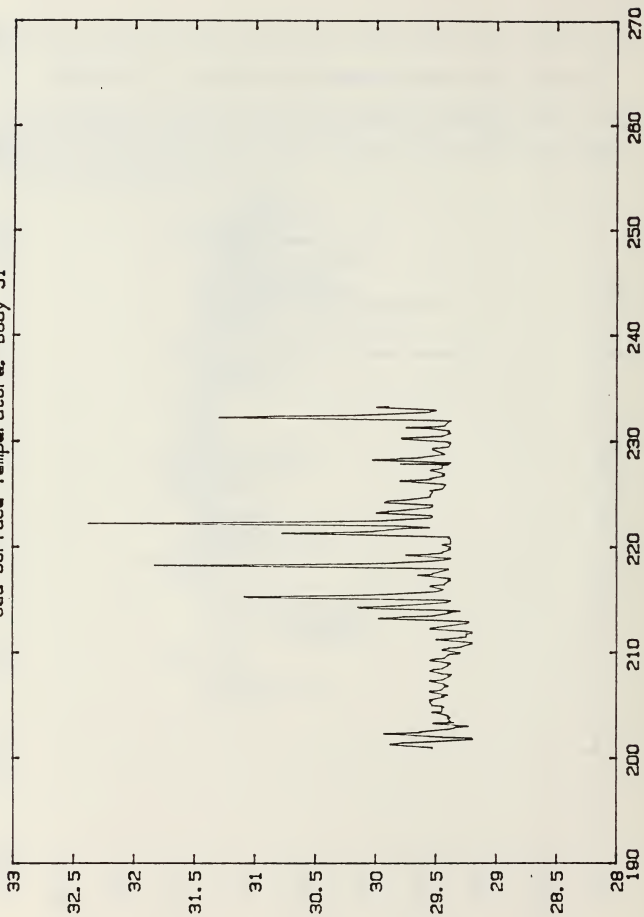
STATION: 128 LAT: 1 15.3 N  
 DATE: 7/11/88  
 LONG: 130 9.1  
 TIME: 1306Z

## APPENDIX B. LAGRANGIAN TEMPERATURE TIME SERIES

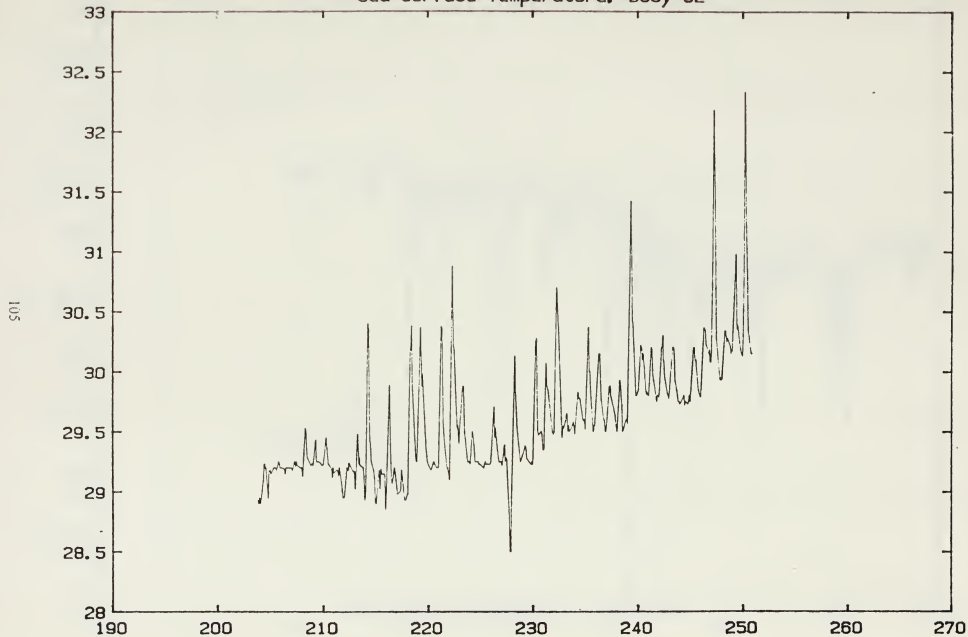
This appendix is included to provide the temperature time series which were discussed in this study and may be of interest to the reader. Also included are the temperature time series based on the raw data.



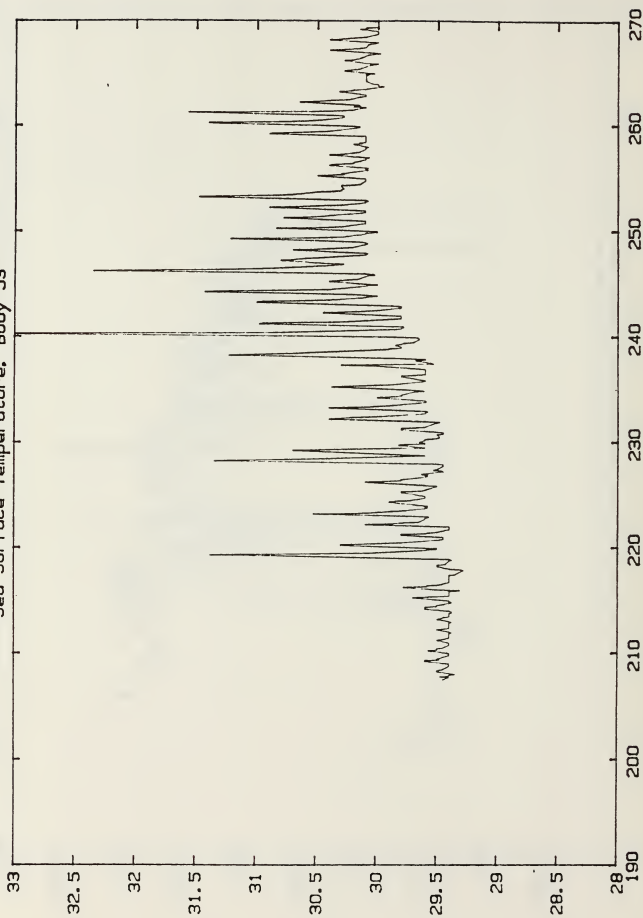
Sea Surface Temperature, Buoy 51



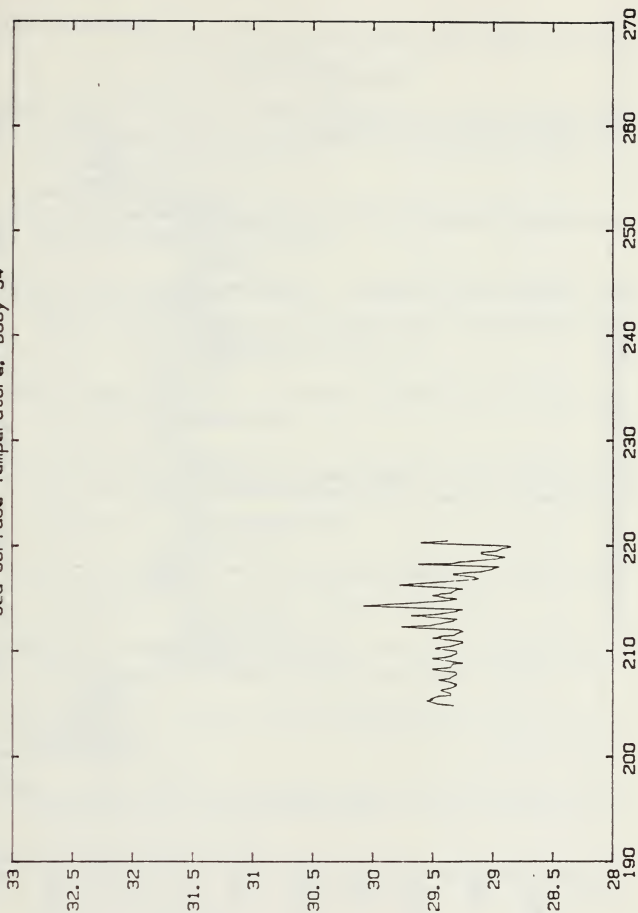
Sea Surface Temperature, Buoy 52



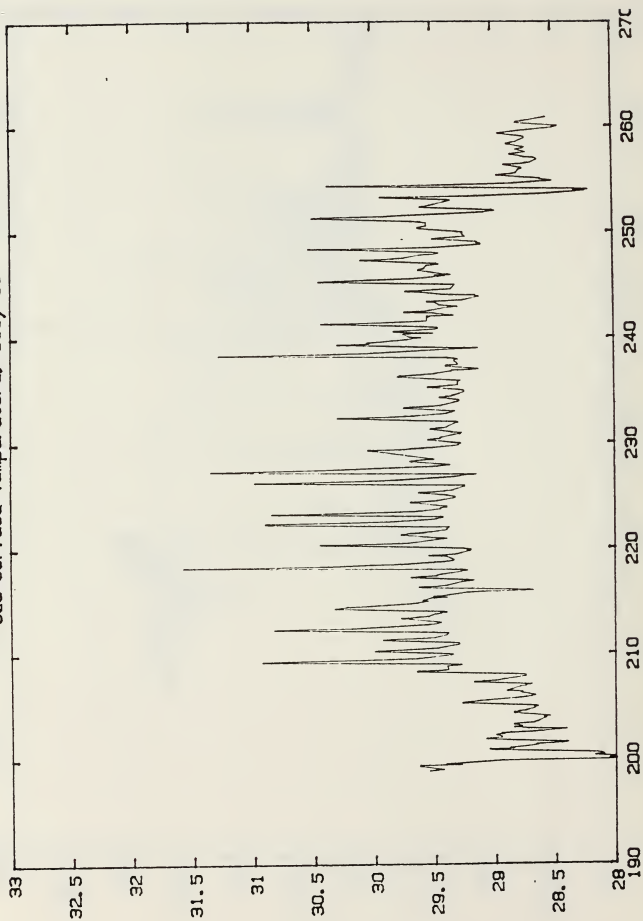
Sea Surface Temperature. Buoy 53



Sea Surface Temperature, Buoy 54



Sea Surface Temperature, Buoy 55



## LIST OF REFERENCES

- Emery, W.J., W.G. Lee, and L. Magaard, Geographic and Seasonal Distributions of Brunt-Vaisala frequency and Rossby Radii in the North Pacific and North Atlantic *J. Phys. Ocean*, 14, 294-317, 1984.
- Cannon, Glenn A., Characteristics of the Waters East of Mindanao, Philippines Islands, August 1965, in *The Kuroshio*, pp. 205-211.
- Lukas, R., Firing, E., Moore, D., Helsley, C. Research Proposal Submitted to the Physical Oceanography Section of the National Science Foundation, *Low-Latitude Western Boundary Currents in the Pacific Ocean*, 1987.
- Niiler, P.P., Davis, R.E., White, H.J., Water-following Characteristics of a Mixed Layer Drifter, *Deep-Sea Res*, 34, 1867-1881, 1987.
- Poulain, P.M., Illeman, J.D., Niiler, P.P., Drifter Observations in the California Current System (1985,1986), *University of California Scripts Institution of Oceanography Data Report*, 1987.
- Takahashi, T., Hydrographical Researches in the Western Equatorial Pacific, *Memoirs of the Faculty of Fisheries Kagoshima University* 7, 141-147, 1959.
- Tsuchiya, M., Lukas, R., Western Equatorial Pacific Ocean Circulation Study (WEPOCS II) *Shipboard Chemical and Physical Data Report*, NSF, 1987
- Wyrtki, K., Magaard, L. and Hager, J., Eddy Energy in the Oceans *J. Geophys. Res.*, 81, 2641-2646, 1976.
- Wyrtki, K. *NAGA Report, Vol. 2: Scientific Results of Marine Investigations of the South China Sea and the Gulf of Thailand*, 1961

## INITIAL DISTRIBUTION LIST

	No. Copies
1. Defense Technical Information Center Cameron Station Alexandria, VA 22304-6145	2
2. Library, Code 0142 Naval Postgraduate School Monterey, CA 93943-5002	2
1. Chairman (Code 63Rd) Department of Meteorology Naval Postgraduate School Monterey, CA 93943-5000	1
2. Chairman (Code 68Co) Department of Oceanography Naval Postgraduate School Monterey, CA 93943-5000	1
3. Professor C. A. Collins (Code 68 Co) Department of Oceanography Naval Postgraduate School Monterey, CA 93943-5000	1
4. Professor Mary Batteen (Code 68BV) Department of Oceanography Naval Postgraduate School Monterey, CA 93943-5000	1
5. Director Naval Oceanography Division Naval Observatory 34th and Massachusetts Avenue NW Washington, DC 20390	1
6. Commander Naval Oceanography Command Naval Oceanography Command Stennis Space Center, MS 39529-5000	1
7. Commanding Officer Fleet Numerical Oceanography Center Monterey, CA 93943	1
8. Commanding Officer Naval Oceanographic Office Stennis Space Center, MS 39522-5001	1

9. Commanding Officer  
Naval Ocean Research and Development Activity  
Stennis Space Center, MS 39522-5001 1
  
10. Commanding Officer  
Naval Environmental Prediction Research Facility  
Monterey, CA 93943-5006 1
  
11. Chairman, Oceanography Department  
U. S. Naval Academy  
Annapolis, MD 21402 1
  
12. Chief of Naval Research  
800 North Quincy Street  
Arlington, VA 22217 1
  
13. Office of Naval Research (Code 420)  
Naval Ocean Research and Development Activity  
800 North Quincy Street  
Arlington, VA 22217 1
  
14. LCDR Glen H. Carpenter  
4266 Greensboro Rd  
Corpus Christi, TX 78413 3
  
15. Scientific Liaison Office  
Office of Naval Research  
Scripps Institution of Oceanography  
La Jolla, CA 92037 1
  
16. Library  
Department of Oceanography  
University of Washington  
Seattle, WA 98105 1
  
17. Dr. John Toole  
Physical Oceanography Department  
Woods Hole Oceanographic Institute  
Woods Hole MA. 02543 1
  
18. Research Administration  
Code 012  
Naval Postgraduate School  
Monterey, CA 93943 1
  
19. Professor Klaus Wyrtki  
Department of Oceanography  
University of Hawaii, Manoa  
Honolulu, HI 96822 1
  
20. Dr. Eric Fleming  
Department of Oceanography  
University of Hawaii, Manoa  
Honolulu, HI 96822 1

21. Dr. Roger Lukas 1  
Department of Oceanography  
University of Hawaii, Manoa  
Honolulu, HI 96822
22. Dr. Peter Hacker 1  
Department of Oceanography  
University of Hawaii, Manoa  
Honolulu, HI 96822
23. Dr. Philip Richardson 1  
Physical Oceanography Department  
Woods Hole Oceanographic Institute  
Woods Hole MA. 02543
24. Dr. Rana Fine (Code 68BV) 1  
RSMAS  
University of Miami  
4900 Rockenbacker Causeway  
Miami, FL 33149





Thesis  
C2635 Carpenter  
c.1 Surface circulation  
associated with the  
Mindanao and Halmahera  
Eddies.

Thesis  
C2635 Carpenter  
c.1 Surface circulation  
associated with the  
Mindanao and Halmahera  
Eddies.



thesC2635

Surface circulation associated with the



3 2768 000 82690 3

DUDLEY KNOX LIBRARY